Identification of HIF-1 co-regulators and their modulation in JAK2V617F-driven myeloproliferative neoplasms

Bryce Drylie

Master of Science by Research

University of York

Biology

January 2023

Abstract

This thesis set out to explore HIF-1α:cofactor complexes in the context of a model of JAK2V617F haematological malignancy. This was interrogated by statistical analysis of HIF-1α RIME data, immunoprecipitation, Western blotting, and phospho-flow cytometry. The work presented here indicates that HSPA2 is a specifically non-hypoxic interactor of HIF-1α, whose association with HIF-1α may be induced by TPO and JAK2V617F signalling. Furthermore, experimentation indicates that the hypoxically-induced HIF-1α:NPM1 complex is inhibited by JAK2V617F, and this inhibition may be mediated by JAK2V617F/ERK signalling in normoxia. Aptamer oligonucleotides were investigated as potential modulators of HIF-1α posttranslational modification. Here, an anti-phospho-ERK1 aptamer is shown to bind its target in the nucleus in-vivo by confocal microscopy. The potential of this aptamer as a modulator of ERK function was investigated by flow cytometry, but was not found to modulate ERK1/2 or HIF-1α phosphorylation. In summary, this thesis leaves open the possibility of aptamer-mediated modulation of HIF-1α complexes, indicates HSPA2 as a novel JAK2/JAK2V617F induced HIF-1α interactor in normoxia, and demonstrates the inhibition of the HIF-1α:NPM1 complex by TPO and JAK2V617F signalling and its possible stabilisation by ERK1/2 inhibition in normoxia.

List of Contents

List of Tables

List of figures

Acknowledgements

I would first like to express my deepest gratitude to my primary Supervisor Dr Katherine Bridge for her ongoing support throughout this project, providing technical and theoretical advice, and without whose patience and understanding this thesis would not have been possible. I would also like to give particular thanks to my co-supervisor Prof David Kent, and TAP members Dr Andrew Holding and Prof Ian Hitchcock, whose pertinent feedback during my thesis advisory meetings were invaluable to finding the focus of my project. I am extremely grateful to Dr David Kealy and Dr Cathy Hawley, whose reassurance, and mentoring were pivotal to the development of my skills in the lab. I would also like to express my sincere thanks to members of the Hitchcock group, in particular Dr Julie Ann Tucker, Dr Bianca Rodrigues Lima Ferreira, Dr Zahra Masoumi, and Lucie Moss, to Bridge lab member Abril Arredondo, and to Dr William Grey, all whose willingness to answer questions, aid in locating resources, and encouragement were highly valued during the course of this thesis. I would also like to thank the members of the Biology Technology facility for the training and advice I received throughout my project, and would like to thank all those in the YBRI who provided advice and support throughout my project. Lastly I would like to thank my family and friends for their unending encouragement and support throughout my degree.

Author's Declaration

The final of six biological replicates of the experiments presented in figures 7 and 11 of this work was completed collaboratively with Dr Cathy Hawley as part of preparation for an upcoming paper. I passaged and provided the cells that were then passaged once by Dr Cathy Hawley before the experiment. We then completed drug and antibody treatments of our respective biological replicates (mine the 5th repeat, hers the 6th repeat) in parallel before combining the cells into the same plate for analysis by flow cytometry. The combined data were analysed by myself, and the experiment was of my design. Two washing steps were completed for the 4th repeat of this same experiment by Ruth Ellerington, who did so because she was shadowing me to learn the flow cytometry protocol for use in her project, and for use in preparation of the same upcoming paper that would be continued after I left the lab. This collaborative work is cited as a reference and highlighted in the work where relevant. The unpublished RIME data presented was generated by Dr David Kealy and was analysed by myself. This data is cited as a reference. This encapsulates the collaborative work conducted in the preparation of this thesis. With exception to the above described collaborative work, this thesis is an original work and I am the sole author. This work has not previously been presented for an award at this, or any other University. All sources are acknowledged as References.

1.Introduction

1.1.HIF-1α stabilisation in response to hypoxia

Hypoxia-inducible Factors (HIFs) are transcription factors formed of an α and β subunit, that mediate the cellular response to low partial pressures of oxygen - hypoxia. “Hypoxia”, here, generally refers to oxygen concentrations around 1%, where as an atmospheric concentration of oxygen (of around 20%) is referred to as “normoxia" and the lower concentration of oxygen concentration of around 5% oxygen, such as is found in tissues, being referred to as “physoxia” (McKeown, 2014).The binding of protein factors in cell extracts, which bound upstream of the erythropoietin (*EPO*) gene locus (as demonstrated by EMSA and DNAse protection assay), was an early inkling of hypoxia-inducible transcription (Semenza *et al.*, 1991) With later characterisation by use of reporter constructs, this nuclear factor was characterised as binding specifically to the *EPO* enhancer in hypoxia (Semenza and Wang, 1992) and was termed HIF-1. Further similar experimentation demonstrated that HIF-1 induced activation of *EPO*-enhancer-reporter constructs was induced by hypoxia in cells of differing lineages, and that reporter expression was dependent specifically upon HIF-1 binding the gene enhancer (Wang and Semenza, 1993). HIF-1 was demonstrated, by analysis of the HIF-1α monomer’s co-precipitates to be a heterodimer of an α and a β component (Jiang *et al.*, 1996) Functions of these monomers differ. Both HIF-1α and -1β mRNA expression are unaffected by hypoxia. However, both the protein expression and DNA-binding capacity of HIF-1α are hypoxia-inducible (Eric Huang *et al.*, 1996). Additionally, recombinant expression of chimaeric proteins expressing HIF-1α or -1β -derived protein sequences demonstrated that HIF-1α, and not -1β is the oxygen-sensitive component of the HIF-1 complex (Pugh *et al.*, 1997). Further experimentation supported this theory in demonstrating that HIF-1α is ubiquitinated and targeted to the proteasome for degradation under normoxic conditions. Hence, the importance of post-translational modification in modulation of the hypoxic response was elucidated (Salceda and Caro, 1997; Kallio *et al.*, 1999).

1.2.HIF-1α is a protein whose stability is modulated by posttranslational modification

Of particular interest in regard to HIF posttranslational modification is the hydroxylation of proline residues within HIF-1α. In Normoxic conditions, the proline residues Pro564 and Pro402 of HIF-1α are hydroxylated. This post-translational modification facilitates the binding of the E3-ubiquitylation complex component Von Hippel Lindau (pVHL) to HIF-1α. The binding of this recognition component facilitates HIF-1α’s ubiquitylation and subsequent degradation (Ivan *et al.*, 2001; Jaakkola *et al.*, 2001; Masson *et al.*, 2001; Foxler *et al.*, 2012). Destabilisation of HIF-1α by proline hydroxylation is carried out by prolyl 4-hydroxylases (Berra *et al.*, 2003; Hirsilä *et al.*, 2003; Appelhoff *et al.*, 2004). PHD

proteins require oxygen as a substrate, meaning they act as oxygen sensors (Hirsilä *et al.*, 2003).Of the three PHD proteins identified (PHD1-3), PHD2 is implicated in the cellular response to hypoxia. Upon siRNA mediated knockout of PHD2 protein expression, HIF-1α is accumulated - suggesting that PHD2 is essential for HIF-1α degradation. The same accumulation was not observed for PHD1 or 3 (Berra *et al.*, 2003; Appelhoff *et al.*, 2004). Interestingly, the *phd2* gene is transcribed in response to HIF binding, implying that HIF-1α negatively regulates its own stability (Metzen *et al.*, 2005). PHD proteins hydroxylate proline residues within HIF-1α's oxygen-dependent degradation domain (ODD). However Hydroxylation of an asparagine residue within this domain by the enzyme FIH (factor inhibiting HIF), inhibits the ability of HIF to bind the transcriptional co-activator p300 in a normoxia-dependent manner, meaning that HIF-induced transcription is repressed, providing another form of hypoxia-dependent HIF regulation (Hewitson *et al.*, 2002; Lando *et al.*, 2002). In summary, Hypoxia inducible factors are α-β heterodimeric transcription factors whose α component is sensitive to post-translational modification by a number of oxygen-dependent enzymes.

1.3. Haematopoiesis and haematopoietic stem cells

Haematopoiesis is the process by which all blood cells are produced from haematopoietic stem cells (HSCs), which can entirely recapitulate the blood system of a mouse upon transplantation (Spangrude *et al*. 1988; Jordan and Lemischka 1990) even if just one is transplanted (Osawa *et al*. 1996). Though HSCs (Gekas *et al*. 2005), and potential HSC precursors (Gordon-Keylock *et al*. 2013) have been found in extraembryonic tissues during development , HSCs are thought to be derived from tissues of the embryo proper (Ganuza *et al*. 2018; Cumano *et al*. 2001; Tavian *et al*. 2001) - specifically, cells from the ventral region (Taoudi and Medvinsky 2007; Ivanovs *et al*. 2014) of the dorsal aorta (in mice (de Bruijn *et al*. 2000; de Bruijn *et al*. 2002; Taoudi and Medvinsky 2007) and humans (Ivanovs *et al*. 2011; Ivanovs *et al*. 2014)) - of the aorta-gonad-mesonephros (AGM) (Medvinsky and Dzierzak 1996; de Bruijn *et al*. 2000; de Bruijn *et al*. 2002; Taoudi and Medvinsky 2007). Here, epithelial cells undergo an epithelial to haematopoietic transition (EHT) to become HSCs (Kissa and Herbomel 2010) in a process that requires expression of the gene Runx1 (Chen *et al*. 2009). These HSCs then migrate to the liver, before coming to reside in the bone marrow (Zovein *et al*. 2008).

HSCs are the primary source of blood cells in adults (Sawai *et al*. 2016),and can be divided into two categories: short-term (ST-HSC) and long-term (LT); LT-HSCs can self-renew, but a ST-HSC can only transiently produce all blood lineages (Christensen and Weissman 2001). LT-HSCs tend to be quiescent - only dividing around 4 times throughout the life of a mouse (Bernitz *et al*. 2016). HSCs can self-renew in response to injury to the bone marrow (Wilson *et al*. 2008), and differentiate (Mossadegh-Keller *et al*. 2013; Pietras

et al. 2016) or proliferate (Baldridge *et al*. 2010) in response to inflammatory cytokines. ST-HSCs are thought to differentiate into haematopoietic progenitors (Akashi *et al*. 2000), which are committed to either the myeloid or lymphoid lineages (Kondo *et al*. 1997; Akashi *et al*. 2000) (see Fig.1). In myeloproliferative neoplasm (MPN), this hierarchy changes, mutant JAK2, JAK2V617F (for example) can bias HSCs to differentiate down the myeloid lineage into megakaryocytes (Rao *et al*. 2021), (see Fig.1). In the bone marrow, HSCs have been found to be closely associated with interior bone surfaces (including the trabecular bone and endosteum (Zhang *et al*. 2003)), osteoblasts (Calvi *et al*. 2003) and blood vessels (Kiel *et al*. 2005; Kubota *et al*. 2008). The endothelia of blood vessels of the endosteum are thought to maintain stem cell quiescence (Kunisaki *et al*. 2013; Itkin *et al*. 2016). In addition TPO secreted by osteoblasts near the endosteum secrete TPO, to maintain LT-HSC quiescence (Yoshihara *et al*. 2007). On the other hand, around the sinusoids, stem cell factor (SCF) is secreted by endothelial cells to maintain HSCs, and from leptin-receptor expressing cells to maintain both HSCs and progenitors (Comazzetto *et al*. 2019). Bone marrow stromal cells have also been implicated in expressing the chemokine CXCL12 to maintain HSCs (Greenbaum *et al*. 2013). From this non-exhaustive review, it is clear that haematopoiesis is modulated by the relationship of HSCs to their niche.

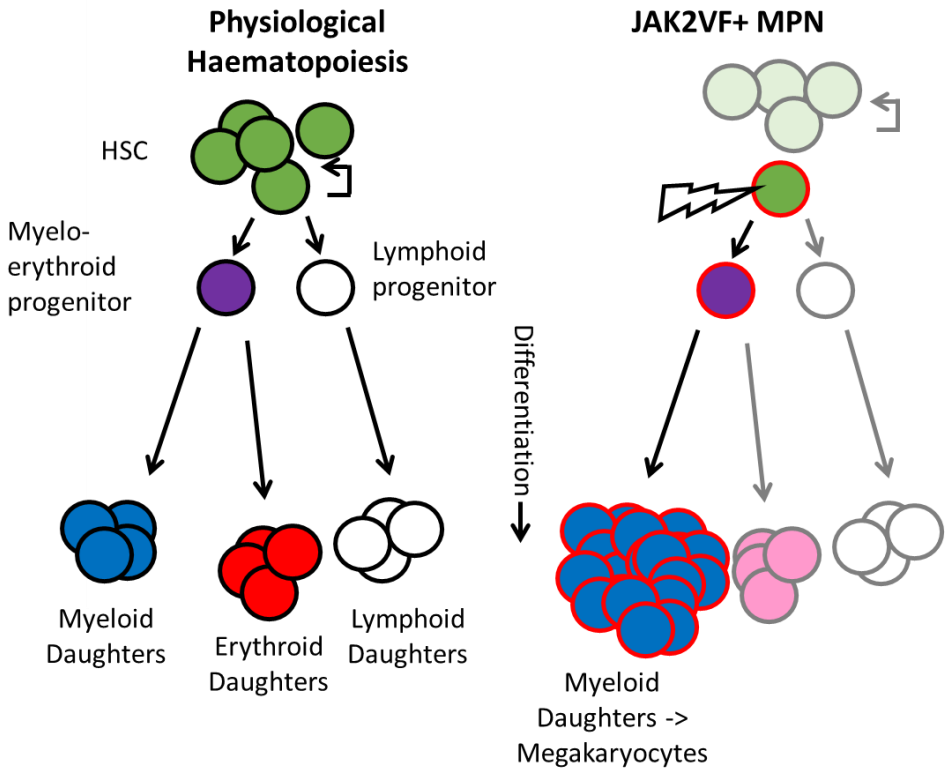

Figure 1: Haematopoiesis in physiological conditions and JAK2V617F+ myeloproliferative neoplasia

A simplified diagram showing the hierarchy of self-renewing HSCs (Christensen and Weissman 2001), and committed Myelo-erythroid/lymphoid progenitors (Kondo *et al*. 1997;

Akashi *et al*. 2000), and how this hierarchy is changed in JAK2VF+ myeloproliferative neoplasia (Rao *et al*. 2021).

1.4.The role of hypoxia in the physiological haematopoietic system

Hypoxia may play a role in haematopoietic stem cell biology. Injection of Hoechst33342 dye into mice has allowed for the stratification of haematopoietic stem cells (HSCs) by their distance from blood vessels in the bone marrow. Such experimentation revealed that cells in regions further from blood vessels (i.e more hypoxic (See Fig.2)) more efficiently repopulated the bone marrow of irradiated mice, suggesting that such cells were long-term HSCs (Parmar *et al.*, 2007; Winkler *et al.*, 2010). Specifically, microscopic analysis has demonstrated that transplanted haematopoietic stem cells (HSCs) hone to the endosteal bone region (Lo Celso *et al.*, 2009; Xie *et al.*, 2009) Of note is that, though the whole bone marrow is hypoxic, local oxygen tension actually increases inverse to distance from the endosteum, but these regions further from the endosteum tend to express nestin protein (Spencer *et al.*, 2014), whose expression on arterial bone-marrow vessels is associated with LT-HSC maintenance (Itkin *et al.*, 2016). And relevantly, nestin expression is associated with HIF-1α stabilisation (Shentu *et al.*, 2020) Furthermore, HSCs maintain HIF-1α stabilisation in normoxic conditions when they migrate from the bone marrow to the peripheral blood (Piccoli *et al.*, 2007). In summary, though hypoxia is important in HSC function, it is also modulated by other factors, and hence, there is disagreement as to the exact role of hypoxia in physiological HSC biology.

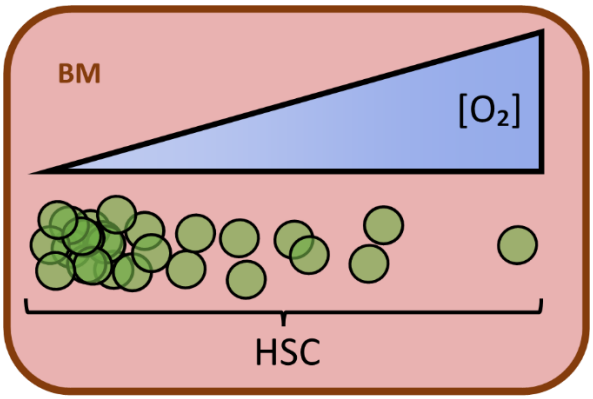

Figure 2: Haematopoietic stem cells are associated with hypoxic regions of the bone marrow:

A schematic to illustrate HSC localisation to a hypoxic niche in the bone marrow (BM) (Parmar *et al.*, 2007; Winkler *et al.*, 2010).

1.5.HIF-1α is implicated in HSC function

Although, as discussed above, the exact function of local oxygen tension in HSC maintenance remains to be elucidated, hypoxia is an established mediator of HSC potential in ex-vivo expansion. Culturing bone marrow extracts in hypoxia better maintains

HSCs in cell culture (Ivanovic *et al.*, 2002; Hermitte *et al.*, 2006; Kovacević-Filipović *et al.*, 2007; Hammoud *et al.*, 2012), and increases the efficiency of HSC transplant in mice (Ivanović *et al.*, 2000; Ivanovic *et al.*, 2004; Shima *et al.*, 2009; Eliasson *et al.*, 2010) by promoting a quiescent LT-HSC phenotype (Shima *et al.*, 2009; Eliasson *et al.*, 2010). A number of studies have implicated HIFs in the maintenance of HSC stemness: Early work on this topic found that Hif-1β-null mice show significantly decreased numbers of haematopoietic progenitors (Adelman, Maltepe and Simon, 1999). In addition, HSCs not expressing pVHL are more quiescent, and show greater transplantation efficiency, suggesting that HIF-1α stabilisation induces HSC quiescence (Takubo *et al.*, 2010). And, that stem cell factor (SCF) signalling, was later found to stabilise HIF in normoxia (Pedersen *et al.*, 2008), Further work has concluded that HIF-1α can protect HSCs from differentiating under oxidative stress, as restoring HIF-1α expression in cells with knocked out *ld2* (whose expression protects from oxidative stress) did just that (Jakubison *et al.*, 2022), but others find that HIF-1α is dispensable for this protective effect (Halvarsson *et al.*, 2019). In conclusion, it appears that there is disagreement as to the role played by hypoxia-inducible factors in the regulation of HSC quiescence.

1.6.Implication of HIF-1α in haematological malignancy

As well as physiological haematopoiesis, HIFs have been implicated as participating in multiple haematological malignancies, including myelodysplastic syndrome (Tong *et al.*, 2012; Hayashi *et al.*, 2018), acute lymphoblastic leukaemia (Benito *et al.*, 2011). And erythroleukaemia (Giuntoli *et al.*, 2007). Furthermore, deletion of HIF-1α has been inhibit the self-maintaining division of leukaemic stem cells (LSCs) in chronic myeloid leukaemia (Zhang *et al.*, 2012) and hypoxia has been implicated in protecting chronic myeloid leukaemic (CML) LSCs from chemotherapy (Giuntoli *et al.*, 2011), and maintenance of stemness in culture (Desplat *et al.*, 2002). In fact, HIF-1α inhibition has been found to induce apoptosis in CML LSCs (Cheloni *et al.*, 2017). Hence, HIFs appear to play an important role in LSC maintenance in CML. There is disagreement, however, as to the role of HIF-1α in acute myeloid leukaemia (AML). On one hand, HIF-1α stabilisation is associated with worse survival in AML patients (Deeb *et al.*, 2011), and AML cells show increased cell cycle arrest under hypoxia (Matsunaga *et al.*, 2012; Drolle *et al.*, 2015), and are more resistant to 12ymptom12rapyy (Drolle *et al.*, 2015). In AML mouse models, HIF inhibition has been associated with improved survival of mice transplanted with AML (Wang *et al.*, 2011) relapsed AML (Y. Wang *et al.*, 2014) and pre-leukaemic AML (Coltella *et al.*, 2015). However, knockout of HIF-1α alone has been found not to affect leukaemogenesis in primarily-transplanted with induced AML cells (Velasco-Hernandez *et al.*, 2014; Vukovic *et al.*, 2015). Furthermore, HIF-1α knockout has been found to quicken the progression of AML symptoms in mice treated with tamoxifen chemotherapy (Velasco-Hernandez *et al.*, 2019). In summary, HIF-1α may have various roles in haematological

malignancies, and there is disagreement as to the role of HIF-1α within some specific malignancies.

JAK2V617F, or JAKVF from here on is a constitutively active mutant of the JAK2 receptor which drives signalling by downstream JAK2 mediator, that is sufficient to cause myeloproliferative disease in mice (James *et al.*, 2005; Sangkhae, Etheridge, *et al.*, 2014), and is found in a large proportion of patients with myeloproliferative neoplasms (Kralovics *et al.*, 2005; Almedal *et al.*, 2016). JAK2VF is relevant to the purpose of this thesis because HIF-1α is stabilised by reactive oxygen species produced as a result of JAK2VF, and drug inhibition of HIF-1α induces apoptosis in JAK2VF-positive cells, suggesting that HIF-1α is a driver of JAK2VF-positive haematological malignancy (Baumeister *et al.*, 2020). In addition, the cytokine thrombopoietin (TPO) can induce HIF-1α stabilisation (Yoshida *et al.*, 2008), and the TPO receptor (MPL) cooperates with JAK2VF, driving haematological malignancy (Sangkhae, Etheridge, *et al.*, 2014). Given that JAK2V617F can drive myeloproliferative neoplasms (James *et al.*, 2005; Sangkhae, Etheridge, *et al.*, 2014) and JAK2VF may stabilise HIF-1α as part of its oncogenic function (Baumeister *et al.*, 2020), JAK2VF provides an ideal model for the study of the function of HIF-1α in haematological malignancy.

1.7.Cofactor-induced modulation of HIF-1α function

HIF-1α function is modulated by cofactors, for example: HIF-1α is directly stabilised by phosphorylation by PIM-1, which promotes angiogenesis in tumours, increasing their growth (Casillas *et al.*, 2021). Of greater significance to the present project, however, is the phosphorylation of HIF-1α by ERK1/2 (Richard *et al.*, 1999). Recent work has demonstrated that HIF-1α's phosphorylation by ERK1/2 induces its association with NPM1, and that that this interaction is required for the nuclear sequestration of HIF-1α, and can affect expression of its target genes (Koukoulas *et al.*, 2021). Given this, it is highly pertinent that ERK1/2 activation is induced by JAK2VF (Wolf *et al.*, 2013; Stivala *et al.*, 2019), as this might suggest that JAK2VF signalling could modulate the formation of the HIF-1α:NPM1 complex, which is induced by ERK1/2's phosphorylation of HIF-1α (Koukoulas *et al.*, 2021). Hence, the possible oncologically-specific modulation of the HIF-1α:NPM1 complex will be investigated in a model JAK2VF-driven haematological malignancy.

The function of HIF-1α cofactors affect HIF-1α function in a context dependent manner: as stated, post-translational modifications as a result of cell signalling can induce HIF-1α transcriptional activity (Casillas *et al.*, 2021; Koukoulas *et al.*, 2021), and more, the heat-shock protein (HSP) HSP90 is required HIF-1α in response to hypoxia (Minet *et al.*, 1999) (but is also a target for the treatment of JAKVF-positive haematological malignancy

(Marubayashi *et al.*, 2010)), whereas the proteins HSP70 and CHIP induce HIF-1α degradation in response to chronic hypoxia (Luo *et al.*, 2010). From these, we can see that HIF-1α activity is highly dependent on cofactors whose activity is itself dependent upon the cellular environment. Hence, it follows that to explore what specific cofactors bind HIF-1α in a specific oncogenic context might reveal mediators of oncogenic HIF-1α function, such as is found in JAKVF-positive haematological malignancies (Baumeister *et al.*, 2020). A molecular biological approach that facilitates such experimentation is RIME (Rapid immunoprecipitation Mass spectrometry of Endogenous proteins). By crosslinking of transcription factors in their active, chromatin-binding conformation with bound proteins, RIME can reveal novel transcription factor cofactors (Mohammed *et al.*, 2013, 2015; Jozwik *et al.*, 2016). Previous (unpublished) work in the Dr Katherine Bridge Lab has applied this technique to HIF-1α in WT JAK2 and JAKVF cell lines in an attempt to elucidate potential oncogenic-specific cofactors in JAKVF-positive haematological malignancies (David Kealy, 2021). Therefore, using statistical analyses, this data will be mined for potential HIF-1α-interactors that are specific to the function of HIF-1α in a model JAKVF-positive haematological malignancy.

1.8.HIF-1α:cofactor interactions as potential mediators of JAK2VF function

JAK2VF-driven haematological malignancies occur when a single HSC acquires a *JAK2V617F* mutation (Van Egeren *et al.*, 2021) leading to the clonal expansion JAK2VF-positive cells, which can occur for over a decade before diagnosis (McKerrell *et al.*, 2017; Van Egeren *et al.*, 2021). JAKVF-positive haematological malignancies can be targeted using JAK2 inhibitors such as Ruxolitinib and Pacritinib (Center for Drug Evaluation and Research, no date; Verstovsek *et al.*, 2010; Raedler, 2015; Singer *et al.*, 2016). Taking the example of Ruxolitinib, the drug improves the symptoms of JAKVF-induced disease in patients, however, it does so whether or not a patient has a haematological malignancy expressing WT JAK2 or JAKVF (Verstovsek *et al.*, 2010). In the case of Pacritinib, the percentage of haematopoietic cells that are JAKVF-positive does not affect a patient's response to treatment with the drug (Verstovsek *et al.*, 2019). Therefore, it follows that researchers have suggested the use of other inhibitors in combination with JAK-targeted therapy to target the aberrant signalling that occurs downstream of JAK2VF (MEK/ERK, JAK/STAT, PI3K/AKT) as an avenue to eradicate the JAKVF-positive clone of cells (Barrio *et al.*, 2013; Khan *et al.*, 2013; Stivala *et al.*, 2019; Brkic *et al.*, 2021) As a whole, and taken together with the possible interactions between JAK2VF, its downstream effects, and HIF-interaction (Wolf *et al.*, 2013; Stivala *et al.*, 2019; Baumeister *et al.*, 2020; Koukoulas *et al.*, 2021) the present research demonstrates that there is a precedent for exploring the therapeutic potential of HIF-1α:cofactor interaction modulation in JAK2V617F haematological malignancies (potential relevant interactions summarised in Fig.3).

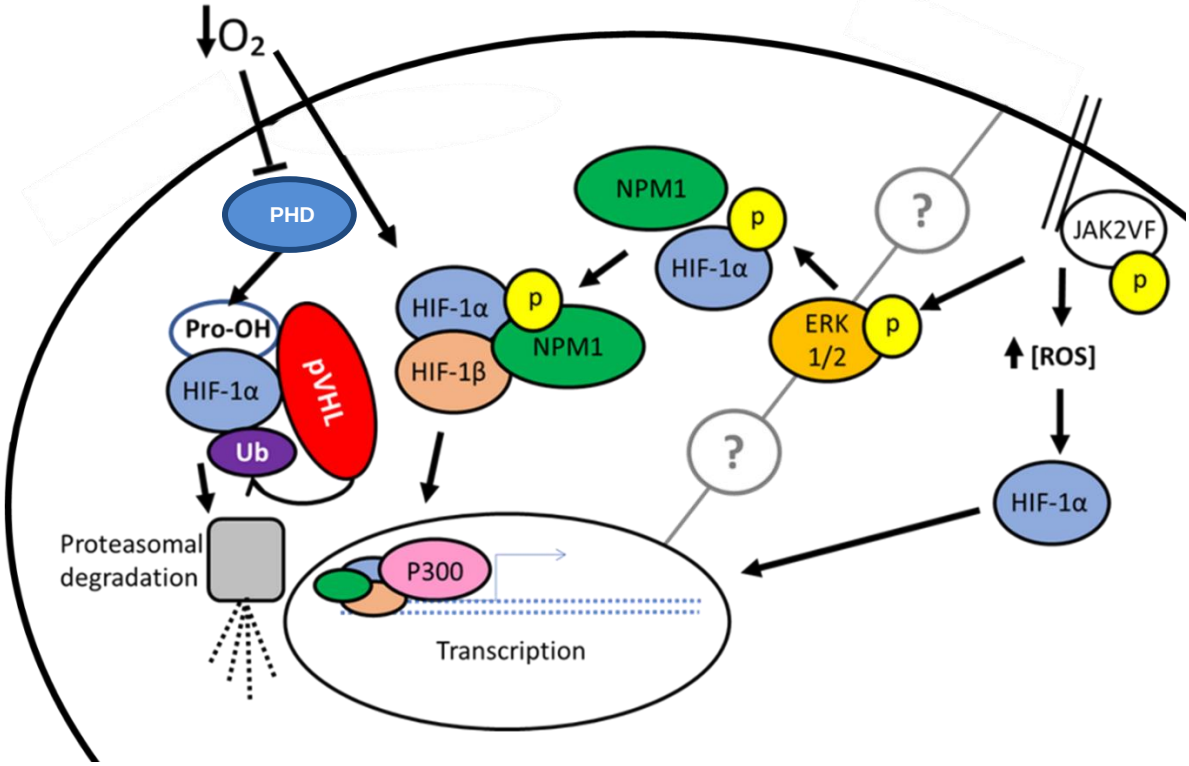

Figure 3: JAK2VF induced signalling could potentially modulate NPM1:HIF-1α complexes

A Schematic representation of relevant mechanisms modulating HIF-1α activity/protein complexes in hypoxia (↓O_2) (Semenza and Wang, 1992, Ivan *et al.*, 2001; Jaakkola *et al.*, 2001; Masson *et al.*, 2001; Foxler *et al.*, 2012, McKeown, 2014, Jiang *et al.*, 1996, Pugh *et al.*, 1997, Hewitson *et al.*, 2002; Lando *et al.*, 2002, Salceda and Caro, 1997; Kallio *et al.*, 1999, Berra *et al.*, 2003; Hirsilä *et al.*, 2003; Appelhoff *et al.*, 2004) and in JAK2VF+ MPN The regulation of ERK1/2 by JAK2VF (Wolf *et al.*, 2013; Stivala *et al.*, 2019) is presented as a possible link between known a JAK2VF:HIF-1 interaction (Baumeister *et al.*, 2020) and HIF-1α complex regulation (Koukoulas *et al.* 2021), marked here as a grey dividing line with question marks (?) within to indicate a hypothetical mechanistic link.

1.9.Aptamer oligonucleotides as potential therapeutic modulators of HIF-cofactor interactions

An avenue for the ablation of oncogenic HIF-1α:cofactor interaction may be oligonucleotide aptamers. Oligonucleotide aptamers are artificially selected to bind to proteins of interest via a process known as SELEX (“Systematic Evolution of Ligands by Exponential Enrichment”) (Tuerk and Gold, 1990). Pegaptanib is an oligonucleotide aptamer therapy (FDA approved in 2004 (US Department of Health and Human Services, 23/March/2005) that functions by binding to vascular epithelial growth factor to the vascular-epithelial growth factor isoform VEGF-165. This aptamer is hypothesised to sterically-inhibit the binding of this disease causing isoform of VEGF to its receptor (Lee *et al.*, 2005), and was used to treat ocular vascular disease (Ng *et al.*, 2006). Pegaptanib

was found to be non-immunogenic (did not induce an antibody response) in a preclinical trial in monkeys (Drolet *et al.*, 2000), whereas a (though note: small) number of cases where anti-VEGF protein-based therapies have been applied have been found to result in inflammation (Souied *et al.*, 2016; Kiss *et al.*, 2018). Therefore, this data suggests that an advantage of aptamers is their non-immunogenicity. In addition, aptamers can be taken up by cells via macropinocytosis or endocytosis (Reyes-Reyes, Teng and Bates, 2010; Yu *et al.*, 2013). Therefore, another advantage of aptamer therapies is their ability to access intracellular targets. Given the avenue for modulating the downstream effects of JAK2VF that HIF-1α provides (Wolf *et al.*, 2013; Stivala *et al.*, 2019; Baumeister *et al.*, 2020; Koukoulas *et al.*, 2021), and that HIF-1α function is endogenously modulated by long non-coding RNA binding in cancer (Shih *et al.*, 2017), it would be biologically informative to study the effects of an anti-HIF-1α aptamer upon the formation of JAK2VF-induced oncogenic complexes and/or resulting post-translational modifications. Unfortunately, there are no known commercially available anti-HIF-1α aptamers at the time of writing. However, there does exist an anti-phospho-ERK1 aptamer (Base Pair, ATW0092). ERK1/2 is relevant to both JAK2VF (Wolf *et al.*, 2013; Stivala *et al.*, 2019) and HIF-1α biology (Richard *et al.*, 1999; Koukoulas *et al.*, 2021). Therefore, the effects of this oligonucleotide upon the potential downstream effects of JAK2VF signalling upon the interaction of ERK1/2 and HIF-1α will be investigated here as proof of principle.

1.10 Aims and Objectives

To summarise, HIF-1α function is modulated by cofactor interactions (Minet *et al.*, 1999; Luo *et al.*, 2010; Casillas *et al.*, 2021; Koukoulas *et al.*, 2021), and may play a role in JAK2VF driven haematological malignancy (Baumeister *et al.*, 2020). JAK2VF can induce signalling (Wolf *et al.*, 2013; Stivala *et al.*, 2019) via known posttranslational modifiers of HIF-1α (Richard *et al.*, 1999; Koukoulas *et al.*, 2021). Specifically, phosphorylation of HIF-1α by ERK1/2 has been shown to modulate HIF-1α interaction with NPM1 via phosphorylation of ERK1/2 (Koukoulas *et al.*, 2021) (see graphical summary, Fig.4). These findings imply the following hypothesis: Oncogenic JAK2V617F/ERK1/2 signalling may induce phosphorylation of HIF-1α, and modulate its interaction with NPM1. Therefore, this project will utilise phospho flow cytometry to assay HIF-1α and ERK1/2 phosphorylation in a JAK2V617F+ background, and apply immunoprecipitation Western blotting to identify whether oncogenic JAK2V617F/ERK1/2 signalling modulates the HIF-1α:NPM1 complex. Additionally, given that a signalling molecule known to be activated by JAK2V617F (Wolf *et al.*, 2013; Stivala *et al.*, 2019) has been shown to modulate HIF-1α:co-factor interactions (Koukoulas *et al.* 2021) implies another hypothesis: JAKV617F signalling may induce HIF-1α to form complexes with cofactor proteins in an oncogenic-specific manner. For this reason, previously unpublished RIME data (David Kealy, 2021) will be mined to identify a candidate oncogenic-specific HIF-1alpha cofactor. Furthermore,

whether this cofactor is an oncogenic signalling (JAK2V617F) specific cofactor will be investigated by immunoprecipitation Western blotting. In addition, ligonucleotide aptamers have been utilised to disrupt protein:protein interactions as therapy (Lee *et al.*, 2005). For this reason, it could be hypothesised that anti-HIF aptamers could target oncogenic HIF:cofactor interactions. Therefore, the ability of a commercially available anti-phospho-ERK1 aptamer (Base Pair, ATW0092) to bind its target *in situ in vivo* will be assessed by microscopy, and effects on ERK1/2 and HIF phosphorylation, which are thought to induce HIF-1α:NPM1 complex formation (Koukoulas *et al.* 2021), will be investigated by phospho flow cytometry. In addition, a DuoLink proximity ligation assay of HIF-1α: HIF-1β interactions will be carried out as proof of principle of a method for investigating the effect of aptamers on intracellular complex formation. The aim of these latter experiments is to serve as proof of principle for the investigation of aptamers as oncogenic HIF-complex targeted therapeutics in JAK2V617F+ MPNs.

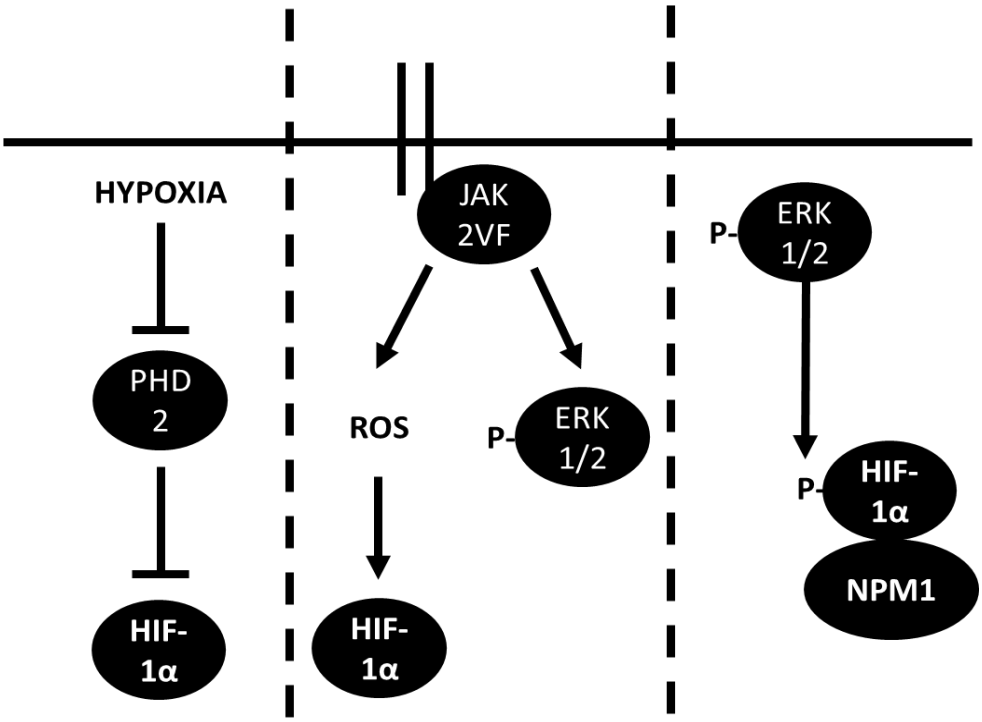

Figure 4: Illustration of relevant HIF-1α modulation mechanisms
Horizontal line marks cell membrane, with components below being intracellular. HIF-1α is stabilised in hypoxia (Salceda and Caro, 1997; Kallio *et al.*, 1999).
and is marked for degradation by PHD2 (Berra *et al.*, 2003; Appelhoff *et al.*, 2004), JAK2VF signalling can stabilise HIF-1α by inducing ROS accumulation (Baumeister *et al.*, 2020) and can activate ERK1/2 signalling (Wolf *et al.*, 2013; Stivala *et al.*, 2019), and ERK1/2 can phosphorylate HIF-1α, inducing its interaction with NPM1 (Koukoulas *et al.*, 2021)

2.Methods

2.1.Culture of hMPL BaF3 and hMPL UT7 cells

Ba/F3-hMPL (referred to simply as Ba/F3) wildtype and JAK2V617F (JAK2VF) cells, as well as WT and VF UT-7/TPO (UT7) cells (cell lines were provided by the lab of Professor Ian Hitchcock) were cultured in R10 medium: RPMI 1640 medium (ThermoFisher 21870076) supplemented with 10% FBS (ThermoFisher A4766), 100 units mL^{-1} penicillin, 100 µg mL^{-1} streptomycin (Gibco 15140130) and 2mM L-glutamine (ThermoFisher 25030081). Ba/F3 cells were also supplemented with 0.5% IL-3 (PeproTech 200-03) and UT-7/TPO cells were supplemented with 10 ng mL^{-1} TPO (Thrombopoietin) (PeproTech 300-18). For starvation, cells were incubated overnight in the same media but with only 2% FBS and no cytokines (herein referred to as R2). For hypoxic treatment, pre-starved cells were placed into a hypoxic chamber (Biospherix, ProOx Oxygen Single Chamber P110) at 1% O^2 for 4 hours unless stated otherwise.

2.2.Statistical analysis of RIME data

A Microsoft Excel spreadsheet of mean spectral counts from 3 biological replicates of a RIME experiment previously carried out upon hMPL UT7/TPO cells was acquired from Dr Katherine Bridge (David Kealy, 2021). These cells had been starved overnight in R2 medium. JAK2V617F cells +/- 100 ng mL^{-1} TPO, then incubated +/- 1% O^2 hypoxia for 4 hours before RIME was carried out. These data were imported as a dataframe into R studio for the calculation of per-condition mean counts, fold-changes between treatment groups, and statistical tests to determine the significance of differences between spectral counts of treatments were analysed in Rstudio (R Core Team, 2021) with additional software packages (Wickham and Bryan, no date; Wickham and Henry, no date; Wickham *et al.*, no date; Henry and Wickham, 2020; Kassambara, 2020; Slowikowski, 2021). Data were organised in Excel (Microsoft, 2011) for analysis and presentation.

2.3.Querying AML data using cBioPortal

Fisher's exact test was carried out by making the following selections in a CbioPortal (Cerami *et al.*, 2012; Gao *et al.*, 2013) query: the Acute Myeloid Leukaemia OHSU 2018 dataset (Tyner *et al.*, 2018) was selected and queried for "Mutations" in the "genomic profiles" section, selecting the 622 "samples with mutation data", and inputting a gene list consisting of "JAK2, NPM1", and copying the table generated in the "Mutual Exclusivity" tab.

2.4.Immunoprecipitations

Cells were starved for 16 hours overnight in 30 mL R2 medium +/- 100 ng/mL TPO (if included) and were incubated +/- 1% O_2 hypoxia for an additional 4 hours, and then lysed in RIPA buffer + 1:100 100x protease inhibitor (Roche 04693159001) and 1µM MG132 (Calbiochem CAS133407-82-6). The day before, Rabbit anti-HIF-1α D1S7W antibody (Cell Signalling #36169) or Rabbit IgG DA1E isotype control (Cell Signalling #3900) were conjugated to streptavidin M-270 Dynabeads (ThermoFisher #65305) at 2 ug mL^{-1} overnight as per the manufacturer's instructions. After washing beads as per the manufacturer's instructions, they were equilibrated in 900 uL of RIPA lysis buffer (150 mN $MgCl_2$, 50 mM Tris-HCL (1M, pH 8.0), 1% Nonidet P-40, 0.5% sodium deoxycholate, 0.1% SDS in ddH_20) and RIPA lysates were added. Lysates and conjugated beads were incubated overnight for 16 hours on a rotary shaker at 30 RPM in 2mL Eppendorf tubes at 4 °C in the dark. Reserves of inputs were left in a 4°C fridge overnight. Following overnight incubation, cells were washed and left in RIPA, then precipitated with a magnetic bar (ThermoFisher 12321D) a total of 7 times. Inputs and lysates were then made up to the appropriate concentrations in denaturing (lysis) buffer (Stewart *et al.*, 2019) (referred to as CLB) with 6.8% β-mercaptoethanol, denatured at 95°C on a heat block in a fume hood before analysis by SDS-PAGE

2.5.Western blot analysis and rapid cell lysate preparation

For rapid lysis followed by western blotting, cell suspensions ($2x10^6$ cells in 2 mL) were aspirated to in 2 mL Eppendorf tubes, spun to a pellet at 4 °C in a microcentrifuge at 2000xg, and the supernatant aspirated and discarded. The pellet was then resuspended in 2 mL PBS+ Protease Inhibitor (Roche 04693159001 - 1 tablet dissolved in 10 mL PBS) and microfuged the same way again. The supernatant was aspirated and the pellet resuspended in 200 uL denaturing (lysis) buffer (Stewart *et al.*, 2019) plus 0.1% MG132, 1% 100x Phosphatase and Protease (Thermo Scientific™ 78441) inhibitor before incubating for 5 minutes on ice. Lysates were briefly mixed by vortexing then heated at 95 °C for ten minutes on a heat block in a fume hood. Lysates were analysed by SDS-PAGE.

40 uL of each sample was loaded into a well of a 10-well 4-20% precast gel (BioRad #4568094) and resolved for ~75 minutes at 120V or until the dye neared the bottom of the gel. Proteins were transferred to PVDF membranes using a Semi-Dry Trans-Blot Turbo system (BioRad 1704150). PVDF membranes were blocked for 10 minutes in EveryBlot blocking buffer (BioRad 12010020) for 10 minutes and incubated with primary antibody (Table 1) in 5% BSA/TBS in a 4 °C cold room with rotation overnight. Membranes were washed the next day 2x 5 minutes and 2x 10 minutes in TBS-T (TBS + 0.05% Tween-20 (Millipore Sigma 9005-64-5)). PVDF membranes were incubated in secondary antibody (Table 2) + 0.02% SDS at room temperature (RT) for 1 hour with rocking. Membranes

were then washed 6x 5 mins with TBS-T and imaged on a ChemiDoc MP imaging system (BioRad 17001402).

Table 1: Primary antibodies used in western blotting:

Primary Antibody Target	Host Species	Supplier	Product name/code	Dilution for blotting
HIF-1α	Rabbit	Cell Signalling	D1SW/#36169	1/1000
HIF-1β	Rabbit	Abcam	ab239366	1/1000
HSPA2	Rabbit	Abcam	ab108416	1/1000
NPM1	Mouse	Fisher Scientific	MA3086/#4TOU-1B2	1/1000
Phospho-ERK (T202/Y204)	Rabbit	Cell Signaling	9101	1/1000
Phospho-HIF1A (S641/ S643)	Rabbit	Antibodies.com	A254482	1/1000

Table 2: Secondary antibodies used in western blotting:

Secondary antibody	Product code	Dilution for blotting
Starbright 520 anti-mouse	BioRad 12005867	1/2500
Starbright 700 anti-rabbit	BioRad 12004162	1/2500
Starbright 520 anti-rabbit	BioRad 12005870	1/2500
Starbright 700 anti-mouse	BioRad 12004159	1/2500
hFAB Rhodamine Anti-Actin Antibody	BioRad 12004164	1/5000

2.6.Microscopy to assess subcellular aptamer localisation

Reconstituted Cy5-tagged Aptamer (ATW0092, Base Pair Technologies) was stored at a concentration of 100 uM in aliquots at -20 °C. Due to small volumes used, aptamer was diluted 1:5 in aptamer resuspension (Base Pair #RTW0001) buffer directly before use before further diluting 1:40 in aptamer resuspension buffer (Base Pair #RTW0003) to a 10x working concentration of 500 nM before boiling for 5 minutes at 95 °C and cooling to room temperature for 15 minutes. Aptamer was then diluted to a final concentration of 50nM in R2 medium supplemented with 1 mM $MgCl_2$. $4.8x10^4$ cells were seeded in 200uL of R2 + 1 mM MgCl2. +/- aptamer for 16 hours overnight in a 96-well v-bottomed flow cytometry plate. The next day, cells were spun down at 300xg for 5 minutes before resuspension in 1 mM MgC_{l2} PBS pre-warmed to 37 °C before spinning down again and then resuspended in 5uM CFSE (ThermoFisher C34554) and 20 nM Hoechst 33342 (Bio-Rad #1351304) in serum free RPMI 1640 + 1 mM $MgCl_2$. The plate was then placed on a plate shaker in the dark at

room temperature for 5 minutes at 200 RPM for 5 minutes before incubating for a further 15 minutes in a 37 °C incubator. Cells were washed again in PBS then resuspended in 180 uL R2 medium. Each 180 uL was split into 90 uL each of an 18 well plate (81817, ibidi) whose wells were pre-washed with PBS to remove any debris. The samples were then moved to an LSM980 microscope (Zeiss) and imaged using an oil immersion lens, with four images being taken per well, for at least 30 minutes total, with each position imaged every 2.5 minutes. After the first 4 time points, 10 uL R2 + MgCl2 +/- 100 ng mL^{-1} TPO was added. Hoechst, CFSE, and Cy5-aptamer were imaged with the H33342, Fcein-T2, and Cy5-T2 channels.

Analysis of aptamer fluorescence was performed in FIJI/ImageJ (Schindelin *et al.*, 2012) using macros generated with the macro recorder tool in imageJ and with reference to acquired from online code resources (Romain Guiet, no date; *imagej.nih.gov*, 2018, *Automate stack splitter frame numbers*, 2020). Timecourse images were split into individual channels using a macro (Romain Guiet, no date), Hoechst and CFSE channels were contrast-enhanced (saturated=90) and normalising and equalising image histograms. Then images were and thresholded to produce masks by running the “Smooth” process x3, then enhancing contrast again (saturated=90, normalise and equalise histogram), then running the “Despeckle” process, and thresholding using the “Otsu dark” method, before converting to a mask by using “Convert to Mask”, using the "method=Otsu background=Dark” options, and running “Fill Holes”. Hoechst33342 masks were used as nuclear masks, and subtracted from CFSE masks to create cytoplasmic masks using the Image Calculator tool. Time Series stacks were then converted to individual images using a macro adapted from code found online (*Automate stack splitter frame numbers*, 2020). Original CFSE masks were inverted to create background masks. Each of the three masks were used to create regions of interest (ROIs) within which the mean grey fluorescence of the Cy5 (aptamer) channel (in raw single images) over time in the nucleus cytoplasm and background. These data were then manually collated in Excel (Microsoft, 2011) and analysed in Rstudio (RStudio Team, 2016) using publicly available code libraries (Wickham and Bryan, no date; Wickham and Henry, no date; Wickham *et al.*, no date; Slowikowski, 2021). For analysis, the mean grey fluorescence intensity was calculated per image in the cytoplasm and nucleus, then mean averages calculated per condition. nuclear/cytoplasmic (N/C) ratios were then calculated (Kelley and Paschal, 2019). The data were then further normalised by subtraction of the initial 4 timepoints (pre +/-TPO treatment) from all timepoints displayed (Goedhart, 2019). Each condition presented was imaged at least 4 times in duplicate (technical repeat wells imaged 4 times in different positions).

2.7.Flow cytometry:

Flow cytometry experiments were performed on a CytoFLEX 355 or CytoFLEX 375 flow cytometer (Beckman Coulter)

2.8.Live cell Flow cytometry

For live cell flow cytometry to assess aptamer uptake Reconstituted Cy5-tagged anti-p202-ERK1) ATW0092 Aptamer (#D5A4Z Base Pair) was prepared as per the manufacturer's instructions to the desired concentration and made up to working concentrations in R2 medium. Cells were incubated in this aptamer-containing medium overnight in stated densities In 200 uL in 96-well v-bottom plates in a 37°C tissue culture incubator. After 16/24hrs, cells were spun down at 300xg in a centrifuge and washed in 37°C PBS. If a live-dead stain was used, Live/Dead Violet (L34958 ThermoFisher) was applied at 1/1000 concentration in 100uL of PBS on ice in the dark for 30 minutes, then the wells were topped up to 200uL with FACS buffer (1% FCS, 2mM EDTA, in PBS), spun down, washed again, and run on the flow cytometer. Compensation and generation of plots was carried out in FlowJo (*FlowJo™ Software - for Windows*, no date).

2.9.Phospho Flow Cytometry

$2x10^5$ cells were seeded per well in R2 medium or R2 containing drug (Table 5) treatment/aptamer (Base Pair technologies, ATW0092) or DMSO/MgCl2/MgCl2+folding buffer concentration-matched controls respectively in a 96-well v-bottom plate. For experiments assessing the effect of TPO stimulation, cells were either incubated overnight in TPO-supplemented R2. The next day, these were were spun down at 300xg at room temperature after 16 hours starvation and resuspended in 50uL TPO + R2 at the concentration used overnight if so, or 25uL of R2 25uL of R2 was then added at twice the intended final concentration to the remaining wells and incubated at 37°C for 15 minutes. Cells were then fixed by adding 16% paraformaldehyde (PFA) to a final concentration of ~2% R2 (i.e 7.5 uL PFA added). After fixation, plates were incubated at room temperature for 15 minutes on a 550 RPM plate shaker, then centrifuged at 400xg for 5 minutes and tipped off. Pellets were resuspended in 200 uL methanol (chilled to -20°C). Plates were then sealed in parafilm and incubated at -80°C overnight. The next day, 60uL of FACS buffer was added to each well and plates spun down at 400*g for 5 minutes before washing again in 200uL FACS. Cells were then incubated in 10uL (unless stated otherwise) of 1x mouse Fc block (BioLegend 101319) for 15 minutes at 4°C. Cells were then resuspended in 50 uL FACS +/- primary antibody (Table 3) and incubated for 1 hour at room temperature at 550 RPM. Cells were then washed in 200uL FACS buffer twice and resuspended in 50 uL FACS +/- secondary antibody (Table 4) as required and incubated in the dark at room temperature for 40 minutes at 550 RPM. Cells were then washed twice again in 200uL FACS and resuspended in 100 uL of FACS before analysing

on the Cytoflex flow cytometer. Compensation, quantification, and dot plots were carried out in FlowJo, and further data analysis completed in Microsoft Excel and Rstudio.

Table 3: Phosflow primary antibodies

Primary Antibody	Product code	Dilution
anti-phospho-ERK1/2 (PE fluorophore) antibody (Thr202/Tyr204)	BioLegend 369506	1/100
Phospho- HIF1A (S641/S643)	Antibodies A254482	1/1000

Table 4: Phosflow secondary antibodies

Secondary Antibody	Product code	Dilution
Starbright 700 anti-Rabbit	BioRad 12004162	1/2500
AF647 Anti-Rabbit	ThermoFisher A-21245	1/1000
AF405 Anti-Rabbit	ThermoFisher A-21245	1/1000

Table 5: JAK2 and MEK inhibitors

Inhibitor	Product code
Ruxolitinib	Cell Guidance systems SM87-10
U0126	Cell Guidance systems SM106-25

*Cells were treated with 2 uM ruxolitinib (Stivala *et al.*, 2019) and U0126 was used at a concentration of 5 uM (Koukoulas *et al.*, 2021) respectively.

2.10.Proximity ligation assay by flow cytometry

$6x10^6$ hMPL Ba/F3 JAK2wt or JAK2V617F expressing cells were seeded in 25mL of R2 medium with +/- 100 ng mL^{-1} TPO for 16 hours. The next day, $5*10^5$ cells from each condition were seeded into 4 wells each of a 96-well plate before spinning at 400xg for 1 minute at 4 Celsius and washing in 200uL Ice cold PBS +2mM EDTA +1:1000 MG132 (1 cOmplete™, EDTA-free Protease Inhibitor Cocktail tablet was dissolved in 10 mL PBS). 200uL FOXP3 fix/perm transcription factor buffer (1:3 dilution of fix-perm to 3 parts diluent) (BioLegend 421403) was added after spinning cells down and mixed by pipetting. Cells were fixed on ice for 45 minutes. Duolink® In Situ PLA® kit (with included buffers) (Millipore Sigma DUO92101) was applied: 1 drop of duolink blocking solution was added to each well and incubated for 60 minutes at 37 Celsius. Cells were then spun down again at 400*g and tipped off before adding 50uL of antibody diluted in Duolink antibody diluent.

Diluent was added alone for probe-only control cells. Plate was incubated overnight at 4 Celsius. The next day, cells were washed in 200uL of Duolink wash buffer A (Sigma-Aldrich, DUO82047). Duolink “Plus” and “Minus” Probes (Millipore Sigma DUO92002, DUO92004) were diluted 1:5 in antibody diluent and 50uL added to each well before incubating for 1 hour at 37 Celsius in a 120 RPM shaking incubator. Duolink Ligation buffer was diluted 1:5 in high purity water and used to dilute Ligase to 1x concentration (1:40). 100uL of diluted ligation buffer was added to each well after spinning down and discarding supernatant as before. Cells were washed in 200uL of wash buffer. Amplification buffer was diluted 1:5 with high purity water and then used to dilute polymerase 1:80. 100uL polymerase+amplification buffer was added to each well after spinning down plate at 400*g and tipping off supernatant. Amplification was carried out overnight, incubating plate at 37 celsius in a 220 RPM shaking incubator. In further steps, the samples were protected from light. Detection buffer was diluted to 1x concentration. Cells were washed twice in 200uL Duolink Wash Buffer and spun down at 400*g and the supernatant tipped off before resuspending in 100uL 1x Detection buffer. Cells were incubated with the detection buffer for 45 minutes at 37 Celsius in a 220 RPM shaking incubator. Cells were spun down and washed twice in 200uL Duolink wash buffer before resuspending in PBS and imaging on flow cytometer (Beckman Coulter, CytoFLEX). The RUNX1 rabbit (Proteintech 25315-1-AP), RUNX1 mouse (Santa Cruz Biotechnologies sc-365644) HIF-1α rabbit (Cell Signaling Technology #36169, and HIF-1β mouse (Abcam Ab2771) antibodies were all used at 10 ug mL^{-1}

3.Results

3.1.HSPA2 coimmunoprecipitates with HIF-1α in a JAK2V617F-dependent manner

RIME (rapid immunoprecipitation mass spectrometry of endogenous proteins) is a technique by which endogenous DNA-bound proteins are cross-linked to their interactant proteins in complex to facilitate identification of novel protein-protein interactions of transcription factors or DNA-binding proteins by mass spectrometry (Mohammed *et al.*, 2013). This technique has previously revealed novel HIF-1α interactors in breast cancer (Yang *et al.*, 2022). A goal of this project was to investigate JAK2VF-specific HIF-1α function. For this reason, unpublished data produced in the Katherine Bridge Lab were analysed. These data were produced via HIF-1α RIME on cytokine-starved hMPL-expressing UT-7/TPO cells in atmospheric normoxia, hypoxia (1% O_2), stimulated with 100 ng mL^{-1} TPO, or expressing the JAK2VF (JAK2V617F) mutant (David Kealy, 2021). The data were then analysed to determine potential novel interactors of HIF-1α (Fig.5a).

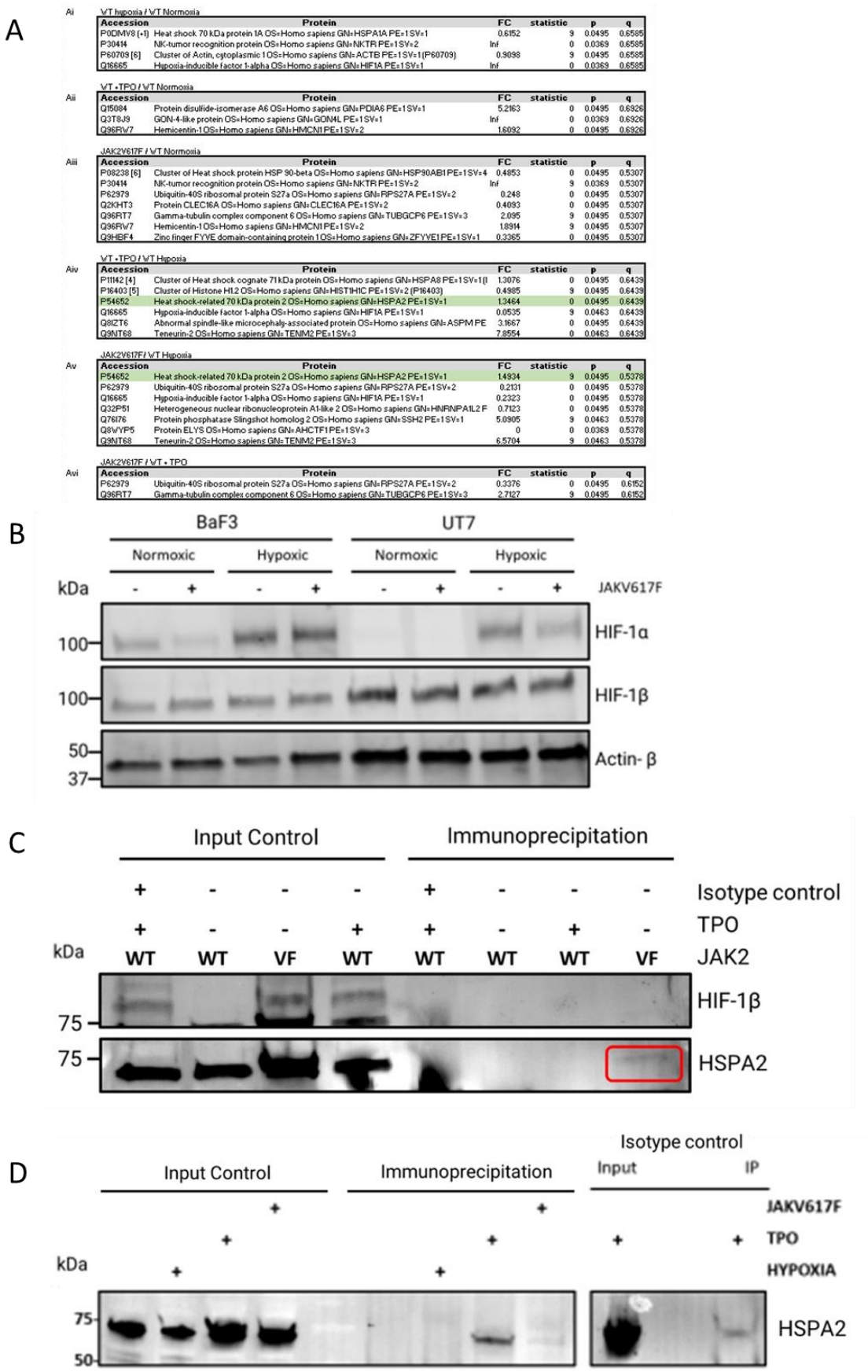

Figure 5: The interaction of HIF-1α and HSPA2 protein increases with TPO stimulation and JAK2V617F:

A; Fold-changes and statistical tests (Wilcoxon Rank-Sum) calculated from spectral counts of proteins co-immunoprecipitated with HIF-1α from UT-7/TPO cells starved in

normoxia, hypoxia (1% O2), stimulated with 100 ng mL^{-1} TPO, or expressing JAK2V617F in the Bridge Lab (David Kealy, 2021). Fold changes were calculated by dividing mean spectra counts (MSC) from each respective protein and condition by their respective MSC in normoxic (i-iii), hypoxic (iv-v), or TPO-treated cells. The statistical significance (p) of these differences was calculated from all 3 biological replicates and Benjamini-Hochberg adjusted for multiple comparisons (q). Those proteins whose expression differed between conditions ($p<=0.05$) are displayed here.

B; A control experiment to demonstrate hypoxic HIF-1α stabilisation in hMPL Ba/F3 or UT-7/TPO cells +/- JAK2V617F. $2x10^6$ per condition were starved for 16 hours in 2mL R2 medium and incubated +/- 1% O_2 hypoxia for a further 4 hours before immediate rapid lysis, analysis by SDS-PAGE, and probing for HIF-1α (D1S7W 1/1000), HIF-1β (ab239366 1/1000) and β-Actin (BioRad 12004164). β-Actin blot is representative of n=2.

C; $6x10^6$ hMPL Ba/F3 cells per condition were starved in RPMI 1640 supplemented with 2% FBS (R2 medium) overnight +/- TPO to a concentration of 100 ng mL^{-1}. Lysates were used for immunoprecipitation with anti-HIF1α D1S7W or a concentration matched IgG DA1E control antibody. Input and precipitate blot (5% and 45% of each lysis loaded respectively) were probed for HSPA2 (1/1000) , then re-probed for HIF1β (1:1000).

D; $100x10^6$ hMPL Ba/F3 cells per condition (each in 4 plates of 30 mL) were R2 medium starved overnight supplemented or not TPO to a concentration of 100 ng mL^{-1}. Starvation was continued for an additional 4 hours and cells were incubated +/- hypoxia (1% O2). Lysates were used for immunoprecipitation with HIF1α or a concentration matched IgG control antibody. 0.5% of lysates were run as input and 40% of IPs were run for blotting. Blots of inputs and precipitates (5% and 40% of each lysis loaded respectively) were probed for HSPA2 protein (1:1000).

Analysis of RIME data using R-Studio indicated that hypoxia and JAK2V617F decrease binding of the heat-shock proteins HSPA1A/HSP70 (*HSPA1A heat shock protein family A (Hsp70) member 1A [Homo sapiens (human)]*, 14-Jan-2023)(FC=0.6172, p= 0.0495, q=0.6585) (Fig.5a i) and HSP90AB1 (FC=0.4853, p=0.0495, q=0.5307) (Fig.5a iii), respectively to HIF-1α compared to normoxia. HSP70 promotes the degradation of HIF-1α (Luo *et al.*, 2010), and HSP90AB1 is an isoform of HSP90 (Mo *et al.*, 2012) thought to be involved in resistance of AML to treatment (Forthun *et al.*, 2012). HSP90-α itself is known to stabilise HIF-1α in an oncogenic context (Tang *et al.*, 2021). Hence, it follows that this analysis of RIME data can highlight novel HIF-1α-interacting proteins.

Given this, it could be suggested that a comparison of RIME data generated in TPO treated and JAK2 V617F cells, or, oncogenic (Sangkhae, Etheridge, *et al.*, 2014; Aynardi *et al.*, 2018) conditions, with hypoxic data might reveal cancer-specific HIF-1α

interactants. Such analysis revealed that more HSPA2 was co-immunoprecipitated with HIF-1α (FC=1.3464, p=0.495, q=0.6439) in TPO-treated (Fig.5a iv) and JAKVF+ (Fig.5a v) cells (FC=1.4934, p=0.0495, q=0.5378) than compared to hypoxia-treated cells. However, none of these differences were statistically significant once corrected for multiple comparisons. Nonetheless, given that this RIME data was preliminary, and HSPs are known to interact with HIF-1α (Forthun *et al.*, 2012; Tang *et al.*, 2021), the prospect of a normoxic TPO/JAK2VF cascade-induced HSPA2:HIF-2α complex was investigated further.

As a prerequisitionary control for the specific effect of hypoxia on hMPL Ba/F3 and UT-7/TPO cells' HIF-1α stabilisation, Western blot analysis was performed to confirm that 4 hours hypoxic treatment (1% O_2) is sufficient to stabilise HIF-1α in these four cell lines (Fig. 5b).

To interrogate the effect of context-dependent formation of an HSPA2:HIF-1α complex in hypoxia, under TPO stimulation, and due to JAK2VF, HIF-1α immunoprecipitation was performed on cytokine-starved Ba/F3 cells (Fig.5c,d). In both experiments, there was an increase in co-immunoprecipitated HSPA2 protein in JAK2VF mutant (Fig.5c,d) or wild-type cells stimulated with TPO (Fig5d), when compared to normoxic or hypoxic cells, but was not co-immunoprecipitated in hypoxia (Fig.5d). Taken together these data corroborate the RIME analysis presented here (Fig.5a), suggesting that signalling via the TPO/JAK2VF cascade is a specific driver of HSPA2:HIF-1α complex formation, which is not formed in hypoxia. However, it is of note that though Figure 5d shows an increase in HSPA2:HIF-1α with TPO stimulation of JAK2 WT Ba/F3 cells, which again corroborates the RIME analysis (Fig.5a.iv), this was not seen in an initial attempt of this same assay (Fig.5c), leaving open the possibility of whether TPO may induce HSPA2::HIF-1α complex formation.

3.2.Optimisation of TPO treatment with regard to HIF-1α and ERK1/2 phosphorylation

The latter RIME experimentation indicated that HSPA2 protein may interact with HIF-1α in response to TPO/JAK2V617F signalling, but not in response to hypoxia. JAK2V617F (Stivala *et al.*, 2019) and TPO can activate ERK1/2 phosphorylation (Gaur *et al.*, 2001). Additionally, ERK1/2 can itself phosphorylate HIF-1α (Richard *et al.*, 1999; Koukoulas *et al.*, 2021). Taken together, these data would support the hypothesis that JAK2VF/TPO stimulation may activate ERK1/2, and ERK1/2 might phosphorylate HIF-1α in turn.

For this reason, the effect of TPO/JAK2V617F upon the phosphorylation of HIF-1α at S641/S643 (targeted for phosphorylation by ERK1/2 (Koukoulas *et al.*, 2021)) was investigated in hMPL Ba/F3 cells. Western blot analysis demonstrated that

phosphorylation of both ERK1/2 and HIF-1α was increased in response to 15 minute and overnight (16hr) 100 ng mL-1 TPO stimulation (Fig. 6a), which is in line with the hypothesis that ERK1/2 activation downstream of JAK2 may induce HIF-1α phosphorylation. To confirm this effect, phospho-flow cytometry was used to investigate the effect of increasing TPO concentration upon ERK1/2 and HIF phosphorylation in WT and JAKVF hMPL Ba/F3 cells (Fig.6a). Though there was an expected increase in ERK1/2 phosphorylation, and JAKVF cells appeared to have higher levels of ERK1/2 overall, there was no effect of either TPO or JAKVF observed on HIF-1α phosphorylation. Given these results, these experiments confirm that TPO/JAK2V617F signalling induces ERK1/2 activation, which may in turn phosphorylate HIF-1α at S641/S643. The contradictory results in the case of pHIF-1α may have been due to the use of a Starbright 700 secondary antibody (BioRad 12004162), which was not known to be optimised for flow cytometry, and not used further. Taking into account the immuno-blotting (Fig.6a) and flow cytometry evidence it was concluded that 10 ng mL^{-1} acute TPO stimulation, or 16 hours at 100 ng mL^{-1} could induce ERK1/2 phosphorylation, 16hrs of 100 ng^{-1} TPO could likely induce HIF-1α phosphorylation, in WT or JAK2VF Ba/F3 cells. Hence, these conclusions were used for further investigation.

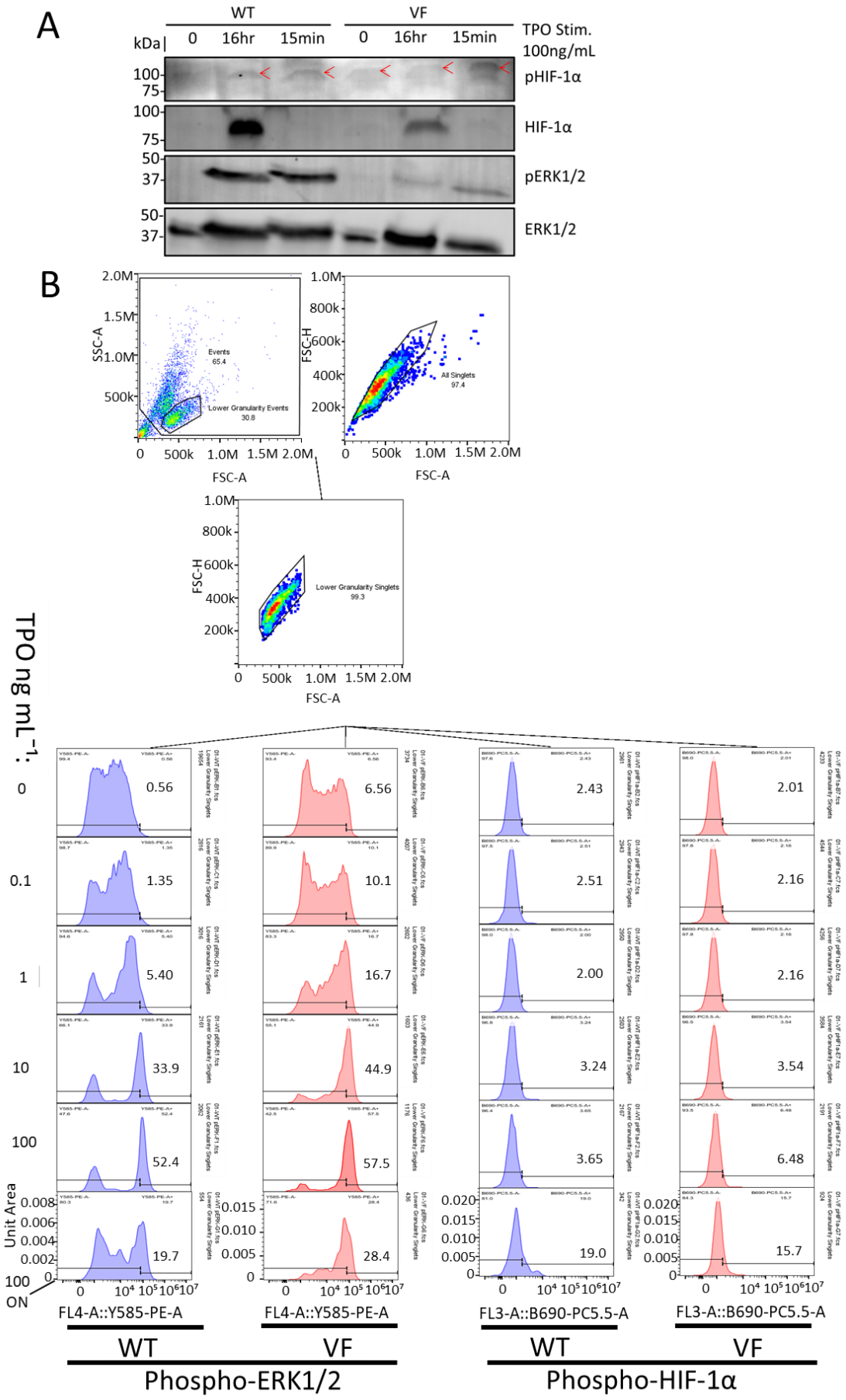

Figure 6: the effect of thrombopoietin concentration and exposure time on the phosphorylation of ERK and HIF-1α:

A; 1 million cells per lane were starved in 180 uL of R2 medium overnight supplemented with +/- 100 ng mL^{-1} TPO. 15 minutes prior to lysis, cells were supplemented with 20 uL R2 supplemented or not with TPO to a final concentration of 0 or 100 ng mL^{-1}. Blots were probed with antibodies raised against total ERK1/2, HIF-1α, phospho-ERK1/2 (phospho sites) or phospho-HIF1a (sites). Red arrows indicate phospho-HIF-1α.
B; $2x10^5$ cells per condition were seeded in 200 ul of R2 with 0 or 100 ng mL^{-1} TPO for 16 hours overnight (100 ON). 15 minutes prior to PFA fixation cells were spun down and resuspended in the final concentration of TPO shown (ON indicates that cells were maintained in that concentration overnight). Samples were probed for pERK (T202/Y204) and pHIF-1α separately, using a starbright 700 secondary antibody to detect pHIF-1α (S641/ S643) levels and left uncompensated as the samples were stained singly and separately. Percentage of singlets expressing either protein is presented as a number to the right of each histogram.

3.3.JAK2V617F may stimulate HIF-1α phosphorylation

To further investigate the role of JAK2V617F in HIF-1α phosphorylation, phospho- flow cytometry was used to assay ERK1/2 and HIF-1α phosphorylation in WT and JAK2V617F hMPL Ba/F3 cells treated with or without the MEK inhibitor (ERK activation inhibitor) U0126 or the JAK2 inhibitor Ruxolitinib. AF647 and AF405 secondary antibodies were used to detect HIF-1α phosphorylation due to the lack of consistency previously observed between assays (Fig.6) in an effort to optimise detection of HIF-1α phosphorylation.

In these assays, and with optimised secondary antibody conditions, JAK2VF cells showed significantly higher ($p=0.0189592$) levels of HIF-1α phosphorylation than WT cells (Fig.7b). There is a trend towards JAK2VF cells having higher levels of phospho-ERK1/2 (Fig.7a,c), with U0126 or Ruxolitinib treatment reducing these to WT-comparable levels. This trend is also seen with HIF-1α phosphorylation (Fig.7b) when an AF647-tagged secondary antibody was used to detect phospho-HIF-1α, but was not observed when an AF405-tagged secondary was used (Fig7d). Overall, these data suggest that JAK2V617F-driven activation of ERK1/2 may lead to phosphorylation of HIF-1α.

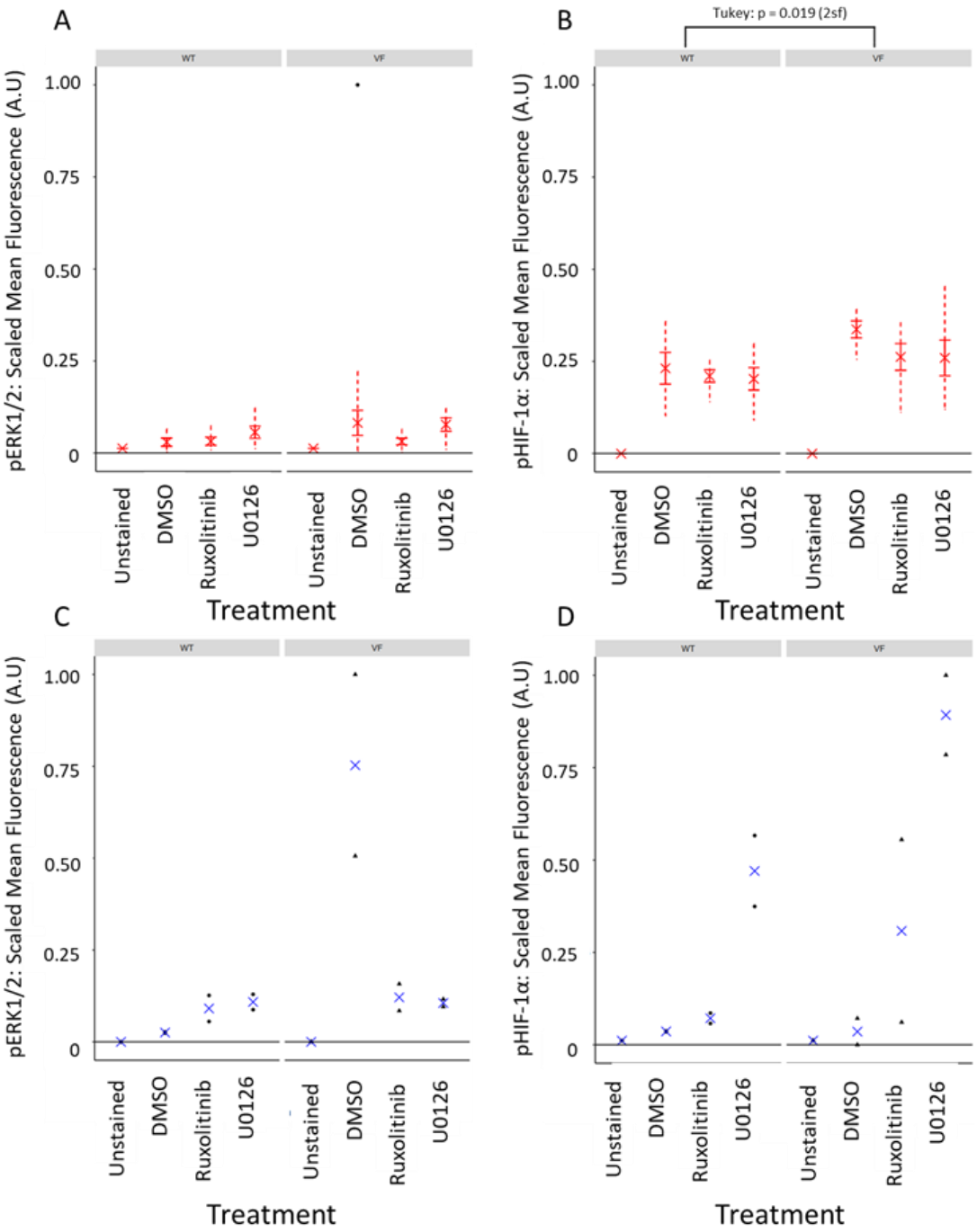

Figure 7: The effect of JAK2 and MEK inhibition upon the phosphorylation of HIF-1α in WT or JAK2V617F hMPL Ba/F3 cells:

A (n=6); Ba/F3 cells were incubated +/- 2 uM Ruxolitinib, or 5uM of U0126 in R2 starvation medium overnight or DMSO control. Cells were fixed with PFA and methanol before probing with anti phospho-ERK. Median fluorescence intensity was mean averaged within biological repeats and background subtracted (unstained samples) before values across samples were scaled to have a minimum and maximum of 0 and 1 across repeats to account for a number of slightly negative values of low staining generated after background subtraction. Red crosses mark biological means with error bars +/- 1 standard error and dotted lines mark the range. Outliers (<25th percentile -1.5*IQR or

>75th percentile + 1.5*IQR) were plotted as black points if within range and not included in calculation of median, SE or range. Statistical analysis was performed in Rstudio. Kruskall-Wallace test showed no statistically significant difference in ERK1/2 phosphorylation between JAK2 genotype/treatment groups ($\chi2 = 7.8859$, df = 5, p-value = 0.1626), Upon outlier removal, Kruskall-Wallace test indicated no significant differences between JAK2 genotype/Treatment ($\chi2 = 6.8921$, df = 5, p-value = 0.2288). Normality was not assumed before outlier removal (Shapiro-Wilk: W = 0.53463, p-value = 1.604e-09), nor after removal (Shapiro-Wilk: W = 0.93408, p = 0.03704).

B; In the same experiment as A, cells were also probed with anti-rabbit AF647-antibody anti-rabbit to detect pHIF-1α. ANOVA was performed to test the effect of JAK2 genotype and inhibitor treatment upon HIF-1α phosphorylation. There was not a significant effect of Treatment (df=2, SS=0.01885, F=1.317, p=0.283), nor an interaction of treatment and JAK2 genotype (df=2, SS=0.00442,F=0.309, p=0.737), but there was a significant effect of JAK2 genotype (df=1, SS=0.04402, F=6.152, p=0.019), which was statistically significant (Tukey test: p=0.0189592). Normality of residuals (Shapiro-Wilk: W = 0.98589, p-value = 0.9176) and homogeneity of variances (Levene's Test: p=0.2001) were assumed.

C (n=2); Ba/F3 cells were incubated without or with 2 uM of Ruxolitinib or 5uM U0126 in R2 starvation medium overnight. Cells were fixed with PFA and methanol before probing with anti pERK-PE. These repeats (including D) were carried out in parallel with those in parts A,B representing the last two repeats. Data were likewise scaled to between 0 and 1 across all samples as with parts A,B.

D; In the same experiment as in C anti-rabbit AF405 antibody was used to to detect anti-pHIF-1α antibody and thus levels of phosphorylation of HIF-1α. Data were treated in the same way as in C.

N.B: Please note that 2 of 6 repeats in A,B and 1 of C,D presented here were produced collaboratively as part of data collection for an upcoming paper (Bryce Drylie, Cathy Hawley, Ruth Ellerington, 2022). Please see Author's Declaration for exact details of this collaboration.

3.4.JAK2V617F and TPO stimulation inhibit the binding of HIF-1α to NPM1, but is rescued by treatment with U0126

ERK1/2 is thought to phosphorylate HIF-1α in hypoxia, inducing interaction with NPM1 (Koukoulas *et al.*, 2021) Having established that JAK2VF may be driving phosphorylation of HIF-1α, it could be hypothesised that JAK2VF may regulate formation of this HIF-1α:NPM1 complex.

NPM1 was coimmunoprecipitated with HIF-1α in starved WT cells at normoxia, and to a lesser extent in JAK2V617F hMPL Ba/F3 cells, but this was abrogated in cells treated with 100 ng mL^{-1} overnight with TPO (Fig.8a), despite higher levels of HIF-1α being

immunoprecipitated in total. HIF-1α levels were higher in immunoprecipitates of DMSO control cells JAK2V617F hMPL Ba/F3 cells compared to WT cells (Fig,8a,b), which was expected as HIF-1α is degraded in normoxia (Salceda and Caro, 1997. Kallio *et al.*1997). These high levels were reduced to a negligible level by Ruxolitinib treatment but not U0126 (Fig.8b). Relative to immunoprecipitated HIF-1α, NPM1 co-IP levels were reduced in VF versus WT cells, but pHIF-1 α levels were level between these groups. Treatment with U0126 overnight partially rescued relative levels of NPM1 co-IP in VF cells, and phospho-HIF-1α levels were greatly increased in proportion (Fig.8c.). When assessed as a whole, these data suggest that JAK2V61F may inhibit the formation of the HIF-1α:NPM1 complex, unlike in hypoxia, and that inhibition of ERK1/2 activity (U0126) may increase HIF-1α phosphorylation and rescue this interaction. This would further suggest that ERK1/2 may contribute towards JAK2VF's inhibition of the HIF-1α:NPM1 complex.
The findings of Koukoulas and colleagues (2021) have suggested that an interaction with the C-terminal domain of NPM1 is necessary for the ERK1/2-induced HIF-1α:NPM1 complex. As was noted int his work, C-terminal NPM1 mutation is associated with NPM1 localisation to the cytoplasm in AML (Falini *et al.*, 2005). JAK2VF also occurs, though rarely, in AML (Levine *et al.*, 2005). With the above discussed data suggesting that JAK2VF signalling may inhibit this complex, this revealed a potential conclusion– that JAK2VF and NPM1 C-terminal mutation may both inhibit the NPM1:HIF-1α complex. To investigate this hypothetical commonality between AML and MPN, therefore, cBioPortal (Cerami *et al.*, 2012; Gao *et al.*, 2013) was used to query a public AML dataset (Tyner *et al.*, 2018). This query demonstrated that NPM1 C-terminal mutation and JAK2V617F mutations were statistically significantly unlikely (Fisher's exact test, p=0.037) to co-occur. This data therefore provides circumstantial evidence that JAK2VF may modulate NPM1: HIF-1α independently of NPM1c mutation (Fig.8d).

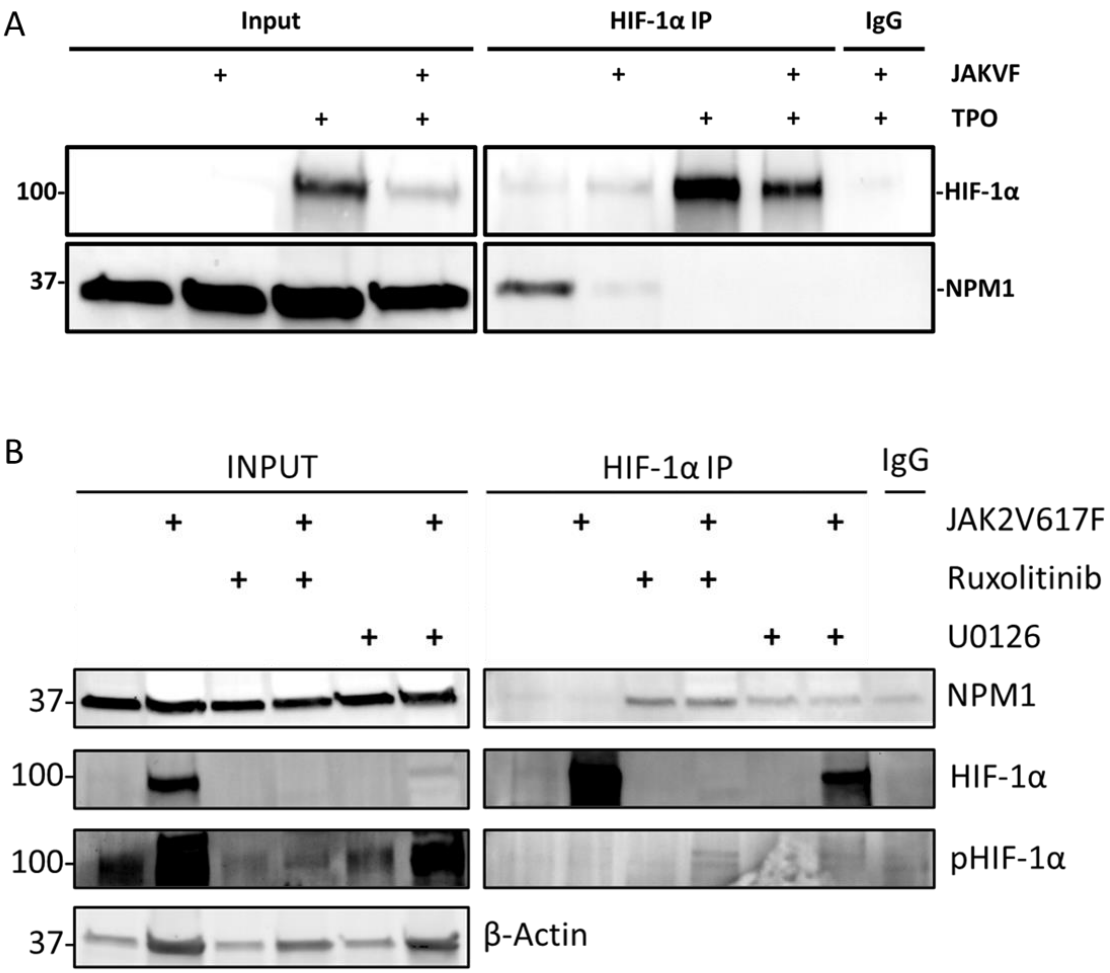

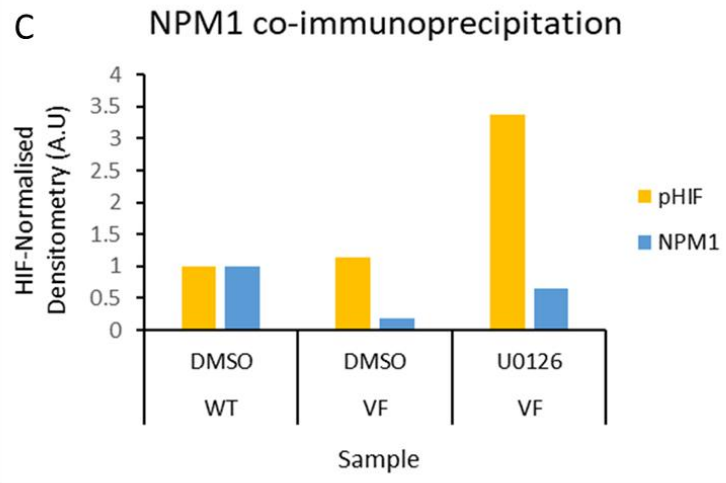

D

A	B	Neither	A Not B	B Not A	Both	Log2 Odds Ratio	p-Value	q-Value	Tendency
JAK2	NPM1	461	26	133	2	-1.907	0.037	0.037	Mutual exclusivity

Figure 8: The effect of JAK2V627F, Ruxolitinib and U0126 treatment on the formation of HIF-1α:NPM1 complexes in hMPL Ba/F3 cells:
A; 10 million cells per condition were starved overnight in R2 +/- 100 ng mL $^{-1}$ TPO. 5% of original lysates were loaded as input and 45% used for immunoprecipitation of HIF-1α. Blots were probed for HIF-1α and NPM1.

B; 10 million cells per condition were starved overnight in R2 supplemented with 2 uM Ruxolitinib, 5 uM U0126, or DMSO control. Each of 6 conditions was lysed in 116.7 uL and 16.7 uL from each pooled for the IgG control. 5% of post-pool lysates were run as input and 45% used for HIF-1α immunoprecipitation.
C; n=2 biological replicates of the conditions as in B quantified as integrated density of blot per lane normalised to HIF-1α in lanes where HIF-1α was expressed.
D; result of a cBioPortal query (Cerami *et al.*, 2012; Gao *et al.*, 2013) of publicly available AML data (Tyner *et al.*, 2018). Fisher's exact test was generated as part of the query, which was to indicate whether or not JAK2 and NPM1 mutations occurred in mutually exclusive groups of patients samples in the dataset.

3.5.Optimisation of cyanine5-tagged anti-pERK1 aptamer uptake in live cells

Aptamers have the potential to act as therapy by modulating intracellular protein interactions (Lee *et al.*, 2005). ERK1/2 is a cytosolic protein that is sequestered to the nucleus upon tyrosine/threonine phosphorylation (Chen, Sarnecki and Blenis, 1992). This provides an avenue to assess the binding of an anti-pERK aptamer (Base Pair, ATW0092) to this protein via its subcellular localisation. Aptamers can be taken up by cells via macropinocytosis and endocytosis (Reyes-Reyes, Teng and Bates, 2010; Yu *et al.*, 2013). Given that ERK1/2 is an intracellular protein (Chen, Sarnecki and Blenis, 1992), it was first essential to assess the ability of anti phospho-ERK1 aptamer (Base Pair, ATW0092) to be taken up by live cells. This was therefore assessed by live cell flow cytometry, and was found to be feasible (Fig.9a-d).

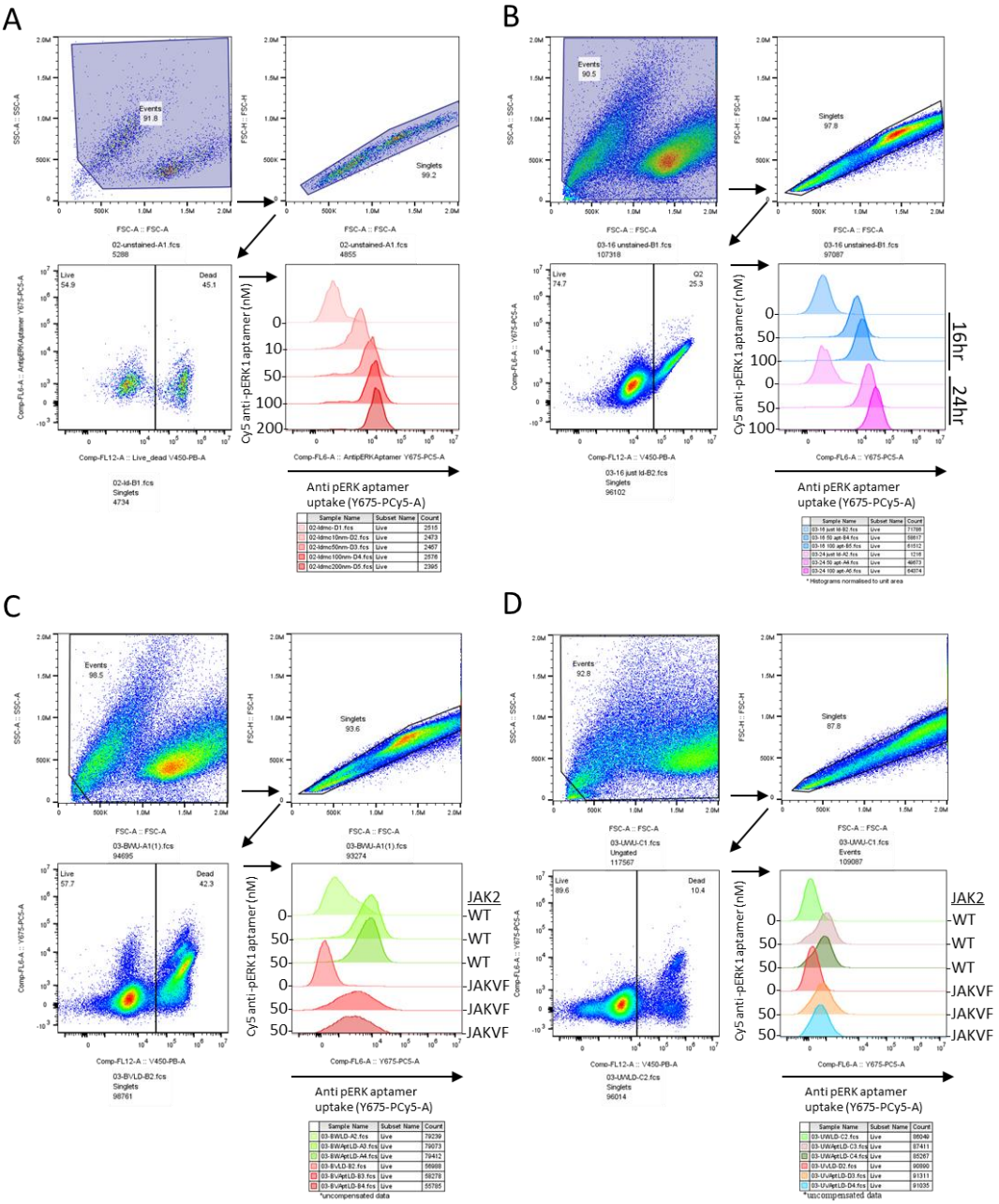

Figure 9: Assessment of uptake of Cy5-tagged anti pERK aptamer with different exposure times and concentrations by live cell flow cytometry:
A; Aptamer uptake in live Ba/F3 hMPL cells under a concentration gradient of cy5-tagged anti pERK1 aptamer after 24hrs. B; Cy5-tagged anti pERK1 Aptamer uptake at 50 and 100 nM after 16 or 24 hrs in Ba/F3 hMPL cells. C; Cy5-tagged anti pERK1 aptamer uptake at 50 nM after 16 hrs in Ba/F3 hMPL cells. D; Aptamer uptake at 50 nM after 16 hrs in live UT-7/TPO cells.

3.6.TPO stimulation of Ba/F3 hMPL cells induces nuclear import of cyanine5 tagged anti pERK1 aptamer in live cells

With a view to using an anti-pERK aptamer (Base Pair, ATW0092) as a potential ERK modulator, it was essential to establish that the aptamer would bind phospho-ERK in vivo. Therefore, given that: as mentioned, previously, ERK1/2 is usually cytosolic, but

translocates to the nucleus upon being phosphorylated (Chen *et al*. 1992), and ERK1/2 phosphorylation can be induced by TPO signalling (Rojnuckarin *et al*. 1999; Sangkhae *et al*. 2014), it was hypothesised that visualisation of anti phospho-ERK aptamer in-vivo by laser scanning microscopy could demonstrate the sequestration of aptamer to the nucleus upon TPO stimulation of Ba/F3-hMPL cells, which was intended demonstrate the binding of the aptamer to its protein target by proxy.

From visual inspection, the fluorescence of nuclei of Ba/F3-hMPL cells treated with Cy5-tagged anti-pERK1 aptamer, TPO stimulation induced aptamer uptake into the nucleus (Fig.10a). In addition, in two biological replicates, the addition of TPO increased the nuclear to cytoplasmic proportion of aptamer (fluorescence) when compared to cells only treated with R2 and no TPO, suggesting that TPO stimulation induced uptake of aptamer into the nucleus in-vivo (Figure 10b). Therefore, these data would suggest that the anti pERK1 aptamer is capable of binding to its stated target in-vivo.

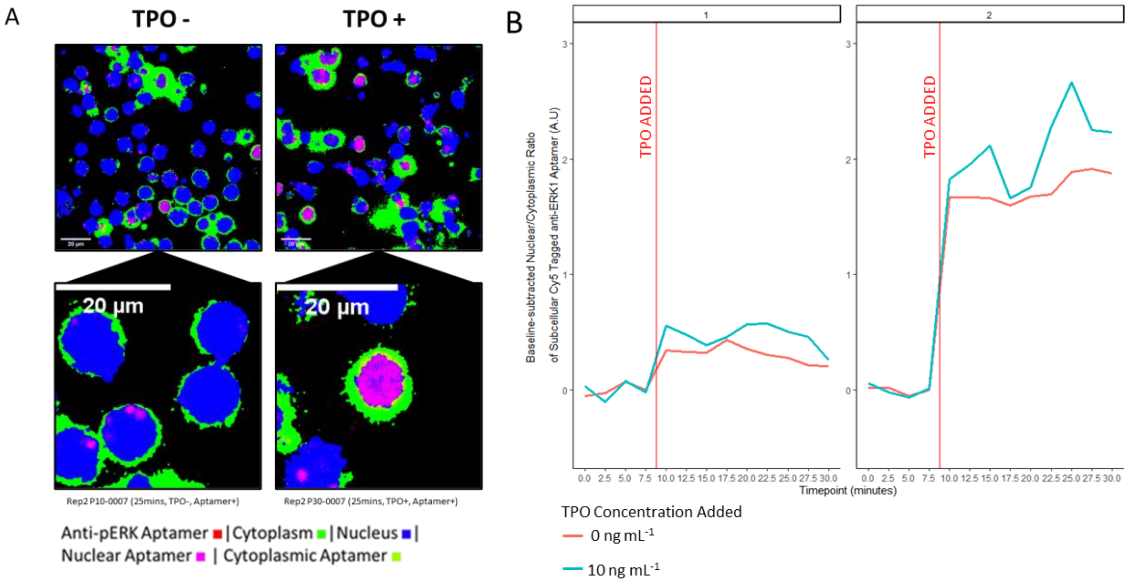

Figure 10: Subcellular localisation of cy5-tagged anti-pERK aptamer over time and in response to stimulation with TPO:

A; Cytoplasmic and nuclear masks presented as composite RGB images with contrast adjusted cyanine-5 channel combined to show Ba/F3/hMPL cells treated with aptamer ~15 minutes after the addition of R2 +/- TPO to a final concentration of 10 ng/mL.

B; Nuclear aptamer (Cy5-tagged Base Pair Technologies ATW0092 aptamer) fluorescence over time before and after adding R2 +/- TPO (final concentration: 10 ng $mL^{-1.}$) to serum-starved Ba/F3-hMPL cells. Background fluorescence was subtracted from cytoplasmic and nuclear data before calculation of normalised nuclear fluorescence as nuclear/cytoplasmic fluorescence ratio (N/C). N/C data was further normalised by subtracting the mean baseline N:C fluorescence (timepoints before TPO addition) from all timepoints before and after TPO addition, per treatment group (+/- TPO group). Both of n=2 biological repeats are presented here.

3.7.Anti-pERK1/2 aptamer does not alter the phosphorylation state of ERK1/2 or HIF-1α.

Given that it appears the anti-phospho-ERK1 aptamer (ATW0092, Base Pair) is capable of binding to its target in-vivo (Fig.10), phospho-flow cytometry was used to assess whether this binding might have an effect upon the phosphorylation of ERK1/2 or the function of phospho-ERK1 with regard to the phosphorylation of HIF-1α.

Treatment of Ba/F3-hMPL cells with cyanine5-tagged anti phospho-ERK1 aptamer (ATW0092, Base Pair Technologies) did not have a statistically significant effect upon the phosphorylation state of phospho-ERK1/2 (Fig.11a) nor the phosphorylation of HIF-1α (Fig.11b). In two repeats of a similar experiment using an AF647-tagged anti phospho-ERK1 aptamer (ATW0092-100, Cambio), and an AF405-anti-Rabbit antibody rather than an AF647 one, there was also no substantial difference in ERK phosphorylation with aptamer treatment. However, in both experiments, there did appear to be a general trend towards greater HIF-1α phosphorylation in WT JAK2 aptamer-treated cells when compared to either DMSO control or $MgCl_2$ loading buffer control.

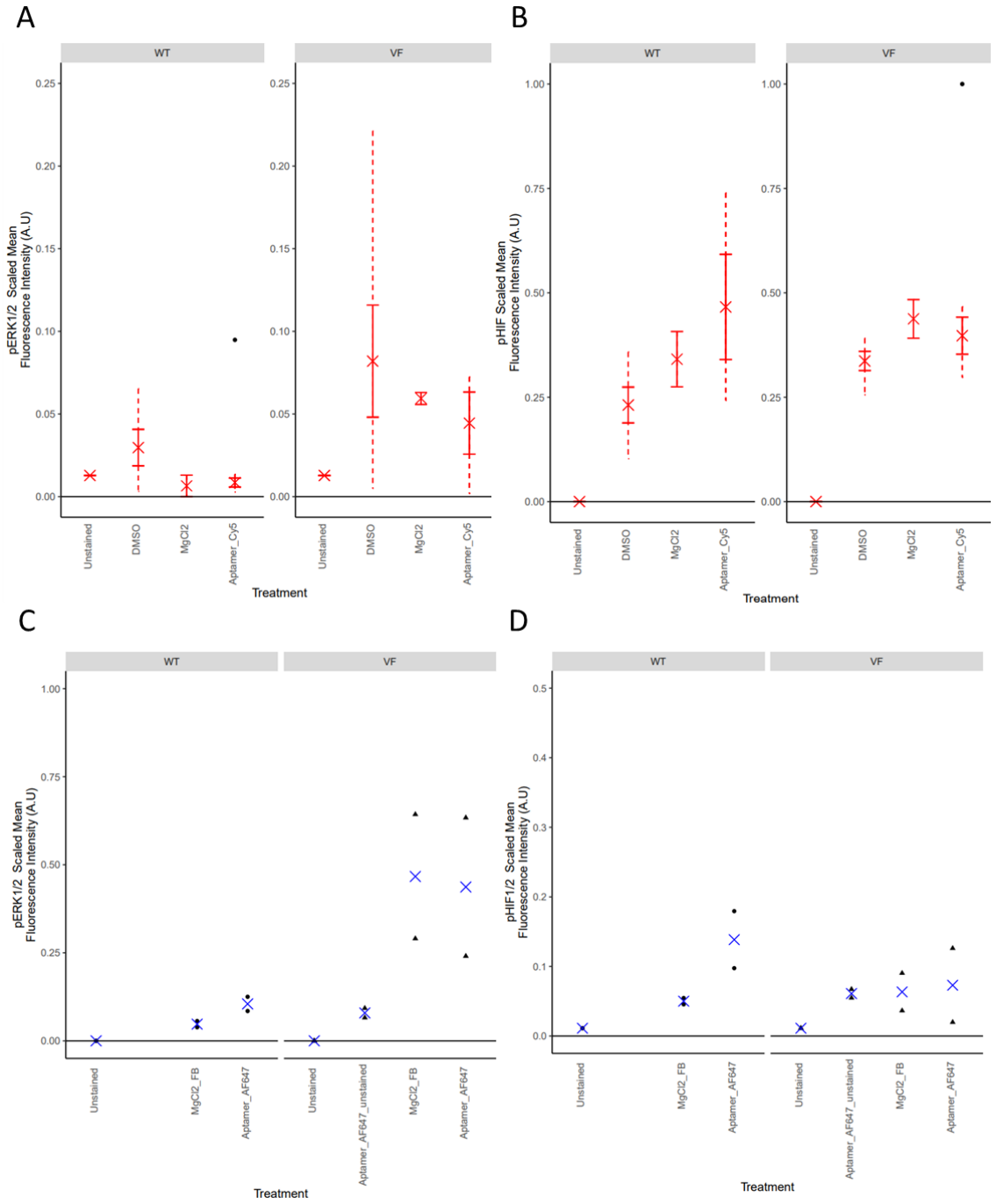

Figure 11: The effect of anti pERK1 aptamer treatment upon the phosphorylation of HIF-1α in WT or JAK2V617F hMPL Ba/F3 cells assessed by phospho flow cytometry: A; Ba/F3 hMPL cells +/- JAK2V617F were incubated with 50 ng mL^{-1} cyanine5-tagged anti pERK1 (Base Pair ATW0092) aptamer overnight in 1mM $MgCl_2$ supplemented R2 or in just R2 + 1mM $MgCl_2$. Panels represent n=4 biological replicates. DMSO controls used in the same biological repeats (n=4) as in figure 7a,b here and in part panel B (run in parallel from the same cell stock) were included to provide a matched control comparison. Median fluorescence intensity was mean averaged within biological repeats and background subtracted (unstained samples) before values across samples were scaled to between 0

and 1. Red crosses mark biological means with error bars +/- 1 standard error and dotted lines mark the range. Outliers (<25th percentile -1.5*IQR or >75th percentile + 1.5*IQR) were plotted as black points if within range and not included in calculation of median, SE or range. ANOVA performed in R showed no significant effect of treatment (df=1, SS=0.000565,F=0.378, p=0.550), nor JAK2 genotype (df=1, SS=0.003350, F=2.243, p=0.160), nor their combined effect (df=1, SS=0.000024, F=0.016, p=0.901). Normality was confirmed by Shapiro-Wilk test (W=0.94999, p=0.4896), and homogeneity of variances confirmed by Levine's test (p=0.952). Outlier removal revealed a marginally significant effect of JAK2 genotype by ANOVA (df=1, SS=0.005565 ,F=4.964, p=0.0477), which was significant by Tukey post-hoc test (p=0.04817). Normality (Shapiro-Wilk: W=0.94438, p 0.4406) and homogeneity of variance (Levine's test: p=0.5368) were assumed. For all statistical tests the $MgCl_2$ treatment group was excluded as it was only included in n=2 repeats.

B; Ba/F3 cells were incubated with 50 ng mL^{-1} -tagged anti pERK1 aptamer (Base Pair ATW0092) overnight in 1mM $MgCl_2$ supplemented R2 or in just R2 supplemented with 1mM $MgCl_2$ as used in aptamer treated samples overnight. Panels represent n=4 biological replicates. An anti-rabbit AF647 (ThermoFisher, 10543623) antibody was used to detect pHIF-1α primary antibody level. Average scaled MFI is presented as in A. ANOVA performed in R showed no significant effect of Treatment (df=1, SS=0.1691, F=4.561, p=0.054), JAK2 genotype (df=1, SS=0.0121,F=0.327,p=0.578), nor their interaction (df=1, SS=0.0008, p=0.884) Upon scaled HIF MFI. Normality (Shapiro-Wilk test: W=0.89853, p-value = 0.07614) and homogeneity of variances (Levene test: p=0.4745). There were also no significant effects of treatment (df=1, SS=0.06917,F=4.406,p=0.0597), nor JAK2 genotype (df=1, SS=0.00090, p=0.8148). Normality (Shapiro-Wilk test: W=0.93359, p=0.3085), and homogeneity of variances (Levene Test: p=0.2078) were assumed. For all statistical tests the $MgCl_2$ treatment group was excluded as it was only included in n=2 repeats.

C: Panel represents MFI (scaled 0-1) of phospho-ERK1/2 PE antibody (Biolegend 369506) used to detect phospho-ERK1/2 levels. Blue crosses are mean averages of MFIs of n=2 biological replicates, both presented as black dots. Ba/F3 hMPL cells +/- JAK2V617F were incubated with 50 ng mL^{-1} AF647-tagged anti pERK1 aptamer (CamBio, ATW0092-100) overnight in 1mM $MgCl_2$ supplemented R2 or in just R2 with 1mM $MgCl_2$ overnight and concentration-matched folding buffer as control. DMSO controls used in the same biological repeats (n=2) as in figure 7c,d here and in panel D (run in parallel from the same cell stock) were included to provide a matched control comparison.

D: Panel represents MFI of AF405 (scaled 0-1) anti-rabbit antibody used to detect phospho-HIF-1α levels, as detected with an anti-phospho-HIF-1α antibody. Blue crosses are mean averages of MFIs of n=2 biological replicates, both presented as black dots. Ba/F3 hMPL cells +/- JAK2V617F were incubated with 50 ng mL^{-1} AF647-tagged anti pERK1 aptamer (CamBio, ATW0092-100) overnight in 1mM $MgCl_2$ supplemented R2 or in just R2 with 1mM $MgCl_2$ overnight and concentration-matched folding buffer as control.
N.B: Please note that 2 of 6 repeats in A,B and 1 of C,D presented here were produced collaboratively as part of data collection for an upcoming paper (Bryce Drylie, Cathy Hawley, Ruth Ellerington, 2022). Please see Author's Declaration for exact details of this collaboration.

3.8.HIF-1 complex formations in small volumes of cells assessed by proximity ligation assay by flow cytometry as proof of principle

Previous assessment of the effects of inhibiting ERK1/2 activation upon formation of the HIF-1α:NPM1 complex (Fig.8), and that ERK can modulate this complex (Koukoulas *et al.*, 2021) left the prospect of using the anti-phospho-ERK1 aptamer (Base Pair, ATW0092) to modulate, the HIF-1α:NPM1 complex - given that the downstream effects of protein:protein interactions have been modulated by aptamer therapies previously (Lee *et al.*, 2005). However, given the cost of aptamers (Base Pair Technologies, ATW0092), and the volumes of cells required for an immunoprecipitation experiment (see methods 2.4) a different protocol would be required to assess the effect of aptamer treatment. The Duolink® In Situ PLA® kit allows for the assessment of protein interactions at the molecular level. Hence it was applied here as a proof of concept for the investigation of HIF-1α:cofactor interactions, such as with aptamers.

PLA by flow cytometry (Fig.12) indicated an increase in HIF-1α:HIF-1β complexes in VF cells compared to WT Ba/F3-hMPL cells, with overnight TPO treatment increasing HIF-1α:HIF-1β complex levels to be in line with those in VF cells. In each case, complex-indicating signal levels were greater than probe-only control. RUNX1 levels were measured by proxy here as a positive control. To measure RUNX1 protein levels, two antibodies (Proteintech 25315-1-AP, Santa Cruz Biotechnologies sc-365644) of different host species, targeted to sequences (Proteintech 25315-1-AP (Proteintech Ag17838), Santa Cruz Biotechnologies sc-365644) of the middle portion same protein (RUNX1) were used as control. The aim of this was to bind two different epitopes of the same protein. This PLA method, instead of detecting interactions between two proteins, therefore indicates the levels of a single protein's expression and is known as "double recognition" (Bonagura *et al*., 2022). RUNX1 is a suitable target for this purpose because it is known to be more highly expressed in JAK2VF-expressing patient samples when compared to healthy controls (Wang *et al*., 2010). Additionally, TPO induced signalling has been

implicated in driving AML expressing the RUNX1 fusion product AML1-ETO (Chou *et al*., 2012; Pulikkan *et al*., 2012). The levels of RUNX1 protein appeared to be increased with both TPO treatment and JAK2V617F, indicating the assay was successful. In future, the small volumes in which cells were analysed (see methods 2.10) could facilitate its use in the investigation of the modulation of HIF complexes by aptamers, given aptamers were previously applied in small volumes for flow cytometric analysis in this project (see methods 2.8/9).

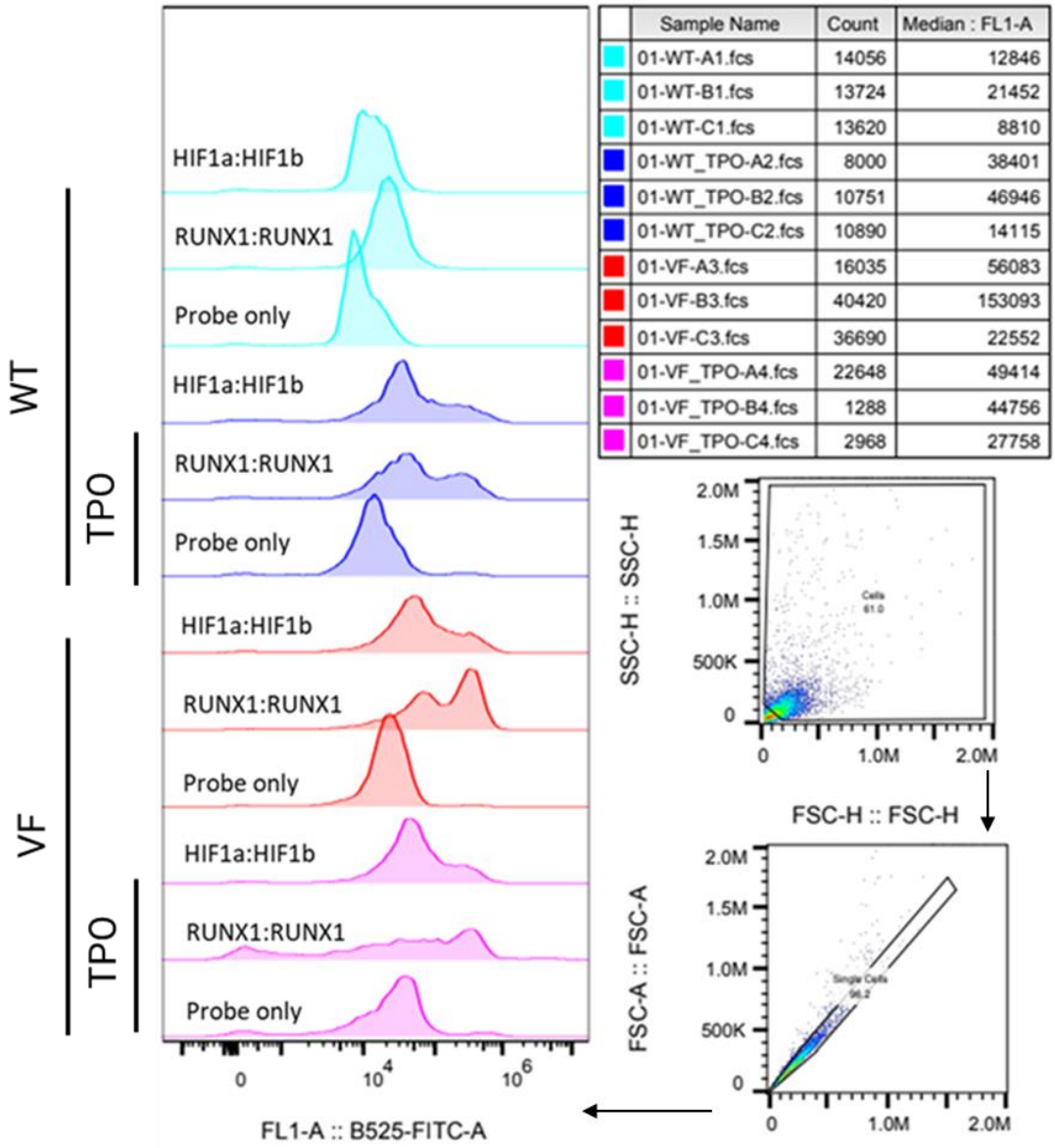

Figure 12: Assessment of HIF-1α:HIF-1β complex formation in Ba/F3-hMPL in response to JAK2V617F and/or TPO treatment:
Cells were starved in R2 medium overnight with or without 100 ng mL^{-1} TPO and fixed. Formation of HIF-1α:HIF-1β complexes in response to TPO and JAK2V617F were assessed by proximity ligation assay by flow cytometry. antibody-untreated cells were treated with PLA probe as a negative control and antibodies of different species to the same RUNX1 protein target were included as a positive control. The experiment represents 1 biological replicate (n=1).

4.Discussion

4.1.JAK2VF drives HIF-1α phosphorylation and inhibits NPM1:HIF-1α interaction in a cell-line model system of JAK2VF-driven haematological malignancy

The results of this project imply that JAK2VF (Fig.8a-c) inhibits formation of the NPM1:HIF-1α complex. In contrast with earlier findings (Koukoulas *et al.*, 2021) ERK1/2 inhibition may drive formation of the NPM1:HIF-1α complex in a JAK2VF mutant background (Fig.8b,c), despite higher HIF-1α phosphorylation (Fig.7b) in cells with this mutant signal transducer. A caveat of these conclusions is that neither a significant effect of JAK2 inhibition, nor effect of the inhibition of ERK phosphorylation upon ERK1/2 or HIF-1α phosphorylation were observed when measured (Fig7). Unexpectedly, use of the ERK1/2 inhibitor U0126 appeared to produce an increase in HIF-1alpha phosphorylation in some of this project's assays (Figs. 7b,d;8c).Of note in this case is that U0126 can act as a reactive oxygen species (ROS) scavenger (Ong *et al.*, 2015), JAK2VF can induce ROS accumulation to stabilise HIF-1α (Baumeister *et al.*, 2020), and, further, ROS accumulation can activate ERK1/2 (Catarzi *et al.*, 2011; Jaenen *et al.*, 2021). With these findings in mind, it is tempting to propose an alternative mechanism wherein ROS accumulation from JAK2VF may modulate HIF-1 α phosphorylation in addition to ERK1/2, but this conclusion cannot be made here and would require further experimentation. However, such a mechanism may explain why U0126 did not appear to have a statistically significant inhibitory effect upon ERK1/2 phosphorylation in JAK2VF cells (Fig.7a). Taken together, these data suggest that JAK2VF drives HIF-1α phosphorylation, but inhibits NPM1:HIF-1α interaction. This finding was not expected, given that ERK1/2-induced phosphorylation of S641/S643 on HIF-1α was previously shown to induce NPM1:HIF-1α interaction (Koukoulas *et al.*, 2021), and that ERK1/2 is activated by JAK2VF (Wolf *et al.*, 2013; Stivala *et al.*, 2019). However, though ERK1/2 activation was increased in control experiments in JAK2VF cells (Fig. 6a,b), there was no statistically significant increase versus WT when tested (Fig.7a) despite data trending to this effect (Fig.7a,c). Overall, these findings suggest that JAK2VF inhibits the NPM1:HIF-1α complex, despite seemingly inducing HIF-1α phosphorylation and may do so in an ERK1/2-independent manner.

TPO can induce ERK1/2 phosphorylation (Gaur *et al.*, 2001), as well as HIF stabilisation (Yoshida *et al.*, 2008). This could imply that TPO, in addition to JAK2VF may modulate the NPM1:HIF-1α complex as has been previously described (Koukoulas *et al.* 2021). Indeed, the assays conducted in this project indicate that prolonged TPO (Fig.6a,b) exposure induces ERK1/2 activation and HIF-1α (Fig.6a) phosphorylation, but as with JAK2VF, TPO stimulation inhibited the NPM1:HIF-1α (Fig.8a) complex. However, one control experiment (Fig.6b) did not recapitulate this result, nor the increase in HIF phosphorylation seen in JAK2VF cells when compared to WT cells that was observed in later experiments (Fig.7b)

This suggests that that the former assay (Fig.6b) may have been limited by the use of a secondary antibody that was not optimised for flow cytometry (BioRad 12004162). When considering these findings as a whole, it appears that prolonged TPO exposure can inhibit formation of the NPM1:HIF-1α protein complex.

Taken together, the findings of the discussed experiments suggest that JAK2 signalling induced by TPO or constitutive activating JAK2VF mutation inhibit the formation of the NPM1:HIF-1α complex, which may have implications for future research. *NPM1* mutation is uncommon in MPN (Montalban-Bravo *et al.*, 2019), but is common in AML, and is associated with cytoplasmic localisation of the protein, rather than nucleolar (Falini *et al.*, 2005) Mutant JAK2VF is uncommon in AML (Levine *et al.*, 2005), but frequent in MPN (M. Wang *et al.*, 2014). In fact, in one patient where both NPM1 mutation and JAK2VF were detected, the mutations were thought to occur different groups of cells (Pasqualucci *et al.,* 2008). Indeed, a query of NPM1 mutations and JAK2 mutations in publicly available data from AML patient samples (Tyner *et al.*, 2018) via cBioportal (Cerami *et al.*, 2012; Gao *et al.*, 2013) demonstrates that JAK2 an NPM1 mutations occur with mutual exclusivity in AML (Fig.8d). In addition, leukaemic localisation of NPM1 to the cytoplasm is driven by mutations in the C-terminal domain of this protein (Falini *et al.*, 2006), which itself is required for formation of the NPM1:HIF-1α complex (Koukoulas *et al.*, 2021). Taken as a whole, these findings may suggest that, modulation of the NPM1:HIF-1α complex by JAK2VF (as investigated here), could possibly occur independently in NPM1-mutated malignancies. If this is the case, NPM1:HIF-1α complex modulation could be a common factor between mutually exclusive (Fig.8d) malignancies, and could be a promising avenue for future research into the molecular biology of haematological malignancies including MPN and AML.

Mutation of the C-terminal domain of NPM1 can cause it to be aberrantly localised to the cytoplasm (NPM1c) (Falini *et al*. 2006), which prevents the differentiation of AML cells to maintain leukaemia. (Brunetti *et al*. 2018). Hence, NPM1c+ AML has been successfully targeted with the drug Eltanexor, which prevents NPM1 export from the nucleus via inhibiting the protein responsible, XPO1 (Pianigiani *et al*. 2022). However, of particular relevance to this work, Eltanexor, and another XPO1 inhibitor, Selinexor, have been successfully applied to JAK2VF MPN cell lines to inhibit growth (Yan *et al*. 2019). Interestingly, the XPO1 inhibitor Selinexor slowed cancer cell line growth in vitro and inhibited HIF-1α induced transcription, but did so without affecting the nuclear localisation of HIF (Depping *et al*. 2019). It has been suggested that NPM1 binds HIF-1α to initiate an oncogenic transcriptional regimen by facilitating increased chromatin binding (Koukoulas *et al*. 2021). However, the findings of this project indicate that NPM1 binding HIF-1α is specifically inhibited the JAK2VF oncogenic signalling background (Fig.8a,b), where HIF-

1α has been shown to actively bind chromatin to induce target gene expression (Baumeister *et al*. 2020), and where HIF-1α is post transcriptionally modified (Fig.7b) in such a way that has been associated with NPM1 binding (Koukoulas *et al*. 2021). Taken together, these data may imply that retention of NPM1 in the nucleus (Pianigiani *et al*. 2022) with HIF-1α (Depping *et al*. 2019), and potentially, therefore, the formation of the NPM1:HIF-1α complex may not be active in JAK2VF+ MPN. However, investigation of the effects NPM1:HIF-1α complex modulation in driving oncogenic phenotype were beyond the scope of the present study. Therefore, further research is needed to determine the effects of NPM1:HIF-1α modulation upon MPN.

To conclude: the data presented in this work implicates JAK2 signalling, whether constitutive, in the form of JAK2VF, or due to TPO stimulation, as a negative regulator of NPM1:HIF-1α interaction, but cannot conclude whether this was induced by JAK2/ERK1/2 signalling inducing HIF-1α phosphorylation. JAK2VF can activate signalling via mediators besides ERK1/2, such as STAT3/5 (Wolf *et al.*, 2013; Hu *et al.*, 2022). Relevantly STAT3 may cooperate with HIF-1α directly to induce transcription (Gray *et al.*, 2005). In addition, HIF-1α can be post translationally modified by mediators besides ERK1/2 to modify its stability (Casillas *et al.*, 2021), and complex formation (Kourti *et al.*, 2015). Therefore, investigation of the effect of downstream JAK2VF target modulation upon the posttranslational modification of HIF-1α and NPM1:HIF-1α complex formation may further elucidate the role of HIF-1α in JAK2V617F-driven haematological malignancies (some possible mechanisms summarised in Fig.13).

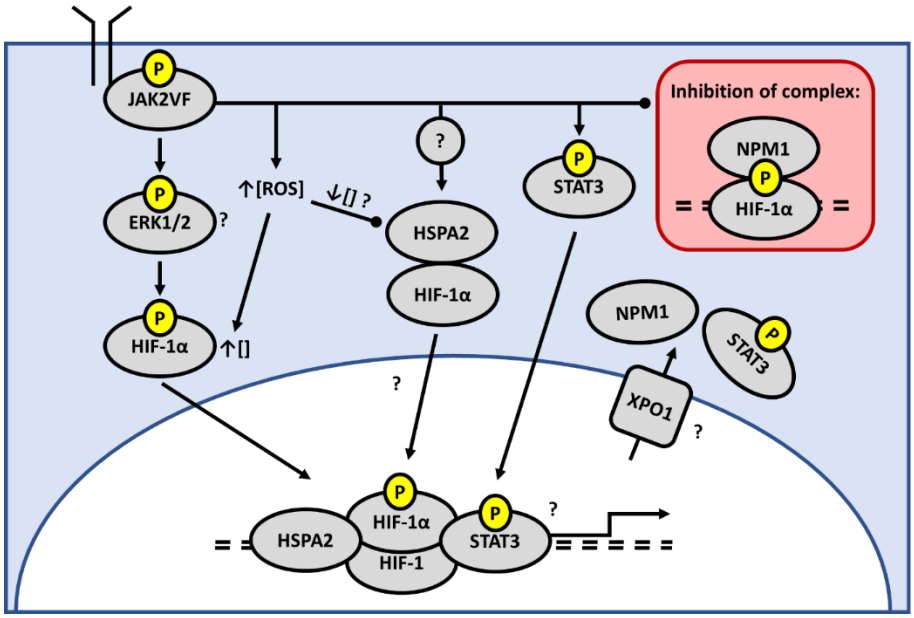

Figure 13: JAK2VF modulates NPM1:HIF-1α and HSPA2:HIF-1α complex formation – a graphical summary in the context of relevant research

This diagram serves as a graphical summary of the mechanisms explored in this project in the context of research discussed above. The findings of this project are presented insofar as JAK2VF may inhibit NPM1:HIF-1α (Fig.8) and induce HSPA2:HIF-1α (Fig.5) binding.

Here JAK2VF/ERK1/2 (Wolf *et al.*, 2013; Stivala *et al.*, 2019), ERK1/2/HIF-1α (Koukoulas *et al.* 2021), JAK2VF/ROS/HIF-1α (Baumeister *et al.*, 2020), JAK2VF/STAT3 (Oku *et al*. 2010), STAT3/HIF (Xu *et al*. 2021, Jung *et al*. 2008), interactions are shown together, this is done for the sake of context and compactness, this is based on separate studies whose results are combined here to summarise the findings of relevant literature, and does not necessarily imply the activity of these mechanisms in consort. Similarly, broader implications made from other literature, concerning the role of XPO1 and ROS/HSPA2 in the modulation of HIF complexes is also hypothetical, and based on inferences from the relevant literature (Bromfield *et al*. 2017,Yan *et al.* 2019, Depping *et al*. 2019, Piangianni *et al*. 2022, Machlus *et al*. 2017). Question marks are used to reflect questions that were beyond the scope of this project e.g. whether JAK2/ERK modulates HIF complexes, the role of ROS in HSPA2 stability in MPN and whether HSPA2 binds HIF-1α in the nucleus and/or cytoplasm, and whether XPO1 (Yan *et al.* 2019, Depping *et al*. 2019, Piangianni *et al*. 2022, Machlus *et al*. 2017) might affect HIF-1α cofactor interactions to modulate gene expression. Further, "[]" represents concentration; downwards in-text arrows represent upregulation; upwards in-text arrows represent down regulation, and yellow circled "P" represents phosphorylation.

4.2.HSPA2 protein is a potential JAK2VF-induced interactor with HIF-1α

Statistical analysis (Fig.5a) of RIME data (David Kealy, 2021) from UT7-TPO Cells expressing WT JAK2 or JAK2 VF indicated that HSPA2 protein was co-immunoprecipitated with HIF-1α in JAK2VF Ba/F3 cells, and those treated with TPO, significantly more so than those WT JAK2 UT7 cells maintained under hypoxia for 4 hours. In this project, assays confirmed that HSPA2 may be a JAK2VF-specific HIF-1α interactant protein (Fig.5c,d), and may too interact with HIF-1α as a result of TPO signalling (Fig.5d). However, these findings come with a number of limitations. Primarily, is the lack of a HIF-1α blot for both immunoprecipitations. This, as was carried out for later experiments (Fig.8) would have allowed for normalisation of protein levels to immunoprecipitated HIF-1α, and quantification of the HIF-1α:HSPA2 interaction. Furthermore, despite use of an optimised immunoblotting protocol applied for control experimentation, which detected HIF-1β in a control experiment in hypoxia in both WT and JAK2VF Ba/F3 cells (Fig5.b), HIF-1β was not detected in hypoxic immunoprecipitates (Fig.5c), despite HIF-1β canonically interacting with HIF-1α under hypoxia, as has been demonstrated by immunoprecipitation (Jiang *et al.*,1996). Given that this dimeric interaction has been well characterised (Jiang *et al.* 1996, Eric Huang *et al.*, 1996), and HIF-1β was detected in input lanes (Fig.5c), it seems likely that this was a technical failure in these samples. Despite the aforementioned limitations, combined, these statistical and in vitro analyses (Fig.5) suggest that HSPA2 physically interacts with HIF-1α in a JAK2VF-dependent manner.

HSPA2 is a protein associated with sperm egg recognition (Redgrove *et al.*, 2012; Gómez-Torres *et al.*, 2022), whose overexpression in cancer has been associated with both worsened (Zhang *et al.*, 2013) and improved survival (Klimczak *et al.*, 2019) in different cancers. Additionally: HSPA2 knockdown has been found to reduce the adhesiveness bronchial epithelial cells, but not non-small cell lung carcinoma cells, leading researchers to suggest HSPA2 drives epithelial differentiation (Sojka *et al.*, 2020). Similarly, knockdown suppressed urothelial cancer line invasiveness, but HSPA2 was not expressed in nonmalignant cells (Garg *et al.*, 2010). HIF-1α has been found to be upregulated in a non-small cell lung cancer cell line (Wei *et al*. 2013) and is associated with worse prognosis in urothelial cancer (Theodoropoulos *et al*. 2004; Basu *et al*. 2021). Contrastingly, HIF-1α is thought to be a driver of epithelial to mesenchymal transition (EMT) in both lung and bladder cancer, to promote invasiveness and metastasis (Liu *et al*. 2018; Zhu *et al*. 2018). Of relevance, JAK2VF has been suggested to upregulate pro-EMT factors to induce myelofibrosis, an MPN (Dutta *et al*. 2017). Considering this data in combination with the present project's findings could therefore imply that HSPA2:HIF-1α is a promising target in JAK2V617F MPN, but more research would be required to determine HSPA2 function in these malignancies. Furthermore, reactive oxygen species (ROS), such as accumulate to stabilise HIF-1α in TPO-stimulated and JAK2VF+ cells (Yoshida *et al*. 2008; Baumeister *et al*. 2020), have been shown to induce HSPA2 degradation in male germ cells (Bromfield *et al*. 2017). Given this, it is interesting that HSPA2 appeared to interact with HIF-1α in JAK2VF, and possibly TPO stimulated cells in the data presented here (Fig.5c,d). It is important to consider that HSPA2 expression can be induced by HIF-1α in cancer cells (Huang *et al*. 2009; Habryka *et al*. 2015), and HIF-1α is thought to protect cells from oxidative stress by reducing production of ROS from mitochondria (Li *et al*. 2019). This is even more pertinent when considering ROS production might contribute to the development of JAK2VF+ MPNs (Marty *et al*. 2013). Therefore, the findings of this project, in the context of relevant past research, may imply a role for HSPA2:HIF-1α complexes in the cellular response to oxidative stress in JAK2VF+ MPNs, though investigation of this was beyond the scope of this study. Another point to consider is that there is precedent for modulation of downstream JAK2VF effectors by a heat shock protein (HSP90) (Fiskus *et al*. 2011), and HSPA2 has been suggested to inhibit ERK1/2 phosphorylation (Cao *et al*. 2019). These findings are, therefore, also suggestive of HSPA2 playing a role in JAK2VF+ MPN (summarised in Fig.13).

4.3.An anti phospho-ERK1 aptamer binds its target in-vivo but does not appear to modulate the phosphorylation state of ERK1/2 nor HIF-1α

Pegaptanib, an aptamer-based therapy, has been shown to inhibit protein function by binding its target protein - possibly functioning via steric hindrance of protein interaction (Lee *et al.*, 2005). Binding of vimentin protein to phosphorylated ERK1/2 sterically hinders

ERK1/2's dephosphorylation (Perlson *et al.*, 2006). Taken together, these findings suggested an anti-phospho-ERK1 aptamer, such as is commercially available (Base Pair, ATW0092) may be able to modulate ERK1/2 function. ERK1/2 is phosphorylated as a result of TPO stimulation (Rojnuckarin, Drachman and Kaushansky, 1999; Sangkhae, Saur, *et al.*, 2014), and undergoes re-localisation to the nucleus from the cytoplasm (Chen, Sarnecki and Blenis, 1992). Corroborating this model, assays employed in the present work indicated that the anti-phospho-ERK1 aptamer was binding its target *in situ* in live cells (Fig.10a,b). However, a limitation of the microscopy approach applied here was that aptamer pre-treatment was previously optimised by flow cytometry for an overnight (16-hour) exposure of aptamer to cells (Fig.9a-b). This could be problematic as aptamers can be degraded within hours in vivo (Kratschmer and Levy, 2017). A direct approach that could be used to confirm aptamer-protein binding is aptoprecipitation, wherein the aptamer is used to purify out its target protein from cell lysates and analysed by Western Blot.(Kim *et al.*, 2014). Such an assay could confirm the ability of the anti-phospho-ERK1 aptamer studied here to bind specifically to its target, in addition to the assay for *in situ* binding presented here.

Given the possibility of using aptamers as therapy (Lee *et al.*, 2005), that ERK1/2 phosphorylation can be maintained by steric hindrance (Perlson *et al.*, 2006), the finding that ERK1/2 can be activated in response to JAK2VF signalling (Wolf *et al.*, 2013; Stivala *et al.*, 2019), and that ERK1/2 may induce an NPM1:HIF-1α complex in hypoxia by phosphorylating HIF-1α (Koukoulas *et al.*, 2021), phospho-flow cytometry was used to assess whether treatment of Ba/F3 WT or JAK2V617F cells with commercially available anti-phospho-ERK1 aptamer (Base Pair, ATW0092) could affect ERK1/2 or HIF-1α phosphorylation. It was found that aptamer treatment did not alter the phosphorylation state of either ERK1/2 or HIF-1α (Fig.11a-d) .However, a limitation of the phospho-flow technique applied to assess the effect of cyanine5-tagged aptamer was that no aptamer-only control was applied to assess whether the fluorophore tag on the aptamer, rather than the antibody fluorophores, may have produced fluorescence (Figs.11a,b), as with the AF617-tagged aptamer experimentation (Figure 11c,d). Yet there still remains the possibility that modulation of HIF:cofactor interaction by aptamer might be better served by employing a different target. STAT3 is activated by JAK2VF (Oku *et al*. 2010), and it has been suggested to be a tumour suppressor in JAK2VF+ MPN (Grisouard *et al*. 2015). Nonetheless, it is of interest here because STAT3 and HIF-1α form a complex in the nucleus bound to chromatin to drive gene expression in cancer (Gray *et al*. 2005), and inhibits the HIF-1α ubiquitination that induces its degradation by directly outcompeting pVHL for HIF1α binding (Jung *et al*. 2008). This is particularly interesting, given that more recent work has suggested that JAK2VF drives STAT3 activation to increase IL-6 production (Li *et al*. 2020). In ovarian cancer, IL-6 expression increases HIF-1α

expression by activating STAT3, and induces HIF-1α to activate oncogene expression in the nucleus (Xu *et al*. 2021). Given the direct nature of the STAT3 interaction with HIF-1α (Jung *et al*. 2008), and oncogenic implications of this that may extend to JAK2VF+ MPN (Li *et al*. 2020; Xu *et al*. 2021; Baumeister *et al*. 2020), STAT3 provides a promising target for HIF-1α:cofactor modulation, as may be achieved by steric hindrance (Lee *et al*. 2005). As discussed earlier, XPO1 inhibitors have been investigated in targeting JAK2VF+ MPN (Yan *et al*. 2019) and oncogenic HIF-1α (Depping *et al*. 2019). This is relevant because XPO1 inhibition can lead to an increase in STAT3 activation in the nucleus upon TPO signalling, and may inhibit HSC differentiation (Machlus *et al*. 2017). Therefore, these findings therefore indicate the potential of HIF-interactor targeted aptamer therapy (summarised in Fig.14), and contextualise the broad implication of aptamer binding a known HIF-1α (Koukoulas *et al*. 2021) interactor in the nucleus (Fig.10).

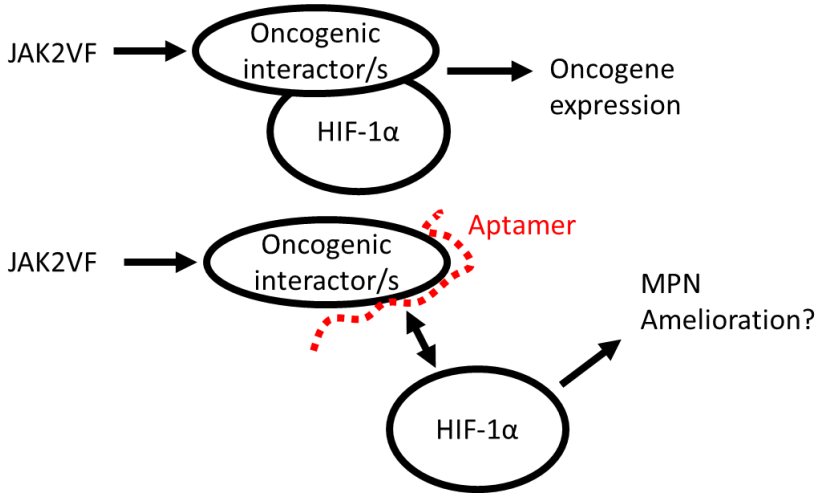

Figure 14: proposed model for modulation of oncogenic HIF-1α coregulators by aptamer as therapy

This project has demonstrated JAK2VF can induce onco-specific HIF-1α:cofactor (Fig.5) interactions, and an aptamer can bind the ERK1/2, a HIF-1α complex modulator (Koukoulas *et al.* 2021) s *in situ* (Fig.10) . Hence, the above diagram proposes a model wherein such cofactors are aptamer-targeted to achieve steric hindrance, as has been targeted as therapy previously (Lee *et al.*, 2005), to oncogenic co-factors, with the aim of ameliorating the possible oncogenic effects of HIF-1α in JAK2VF+ MPN.

Given that ERK1/2 is thought to phosphorylate HIF-1α to induce its complex with NPM1 in hypoxic conditions (Koukoulas *et al.*, 2021), and the above discussed investigation into using anti-phospho-ERK1 aptamer to target ERK1/2 and HIF-1α function, a DuoLink proximity ligation assay (PLA) was carried out as proof of principle (Fig.12) for detecting HIF complexes. Here PLA by flow cytometry demonstrated formation of HIF-1α:HIF-1β complexes in response to TPO and JAK2VF signalling, corresponding with previous works that demonstrated HIF activation by TPO and JAK2VF (Yoshida *et al.*, 2008; Baumeister *et al.*, 2020). Though cells for this experiment were seeded in larger volumes before transferring to a 96-well plate (see methods 2.10),assessments of uptake were carried in

volumes of 200uL in 96-well plates throughout (see methods 2.8/9). In this experiment, the levels of RUNX1 protein were measured by double recognition (Bonagura *et al*., 2022) using two antibodies raised against RUNX1. As expected (Wang *et al*., 2010), RUNX1 levels were increased by oncogenic JAK2VF signalling, which implied a technical success of this protocol. However, though different, both antibodies were raised against regions from the middle portion of RUNX1 (Proteintech 25315-1-AP, Santa Cruz Biotechnologies sc-365644). Given that double recognition PLA attempts to detect protein levels via binding of two different antibodies to different epitopes of the same protein (Bonagura *et al*., 2022), this, therefore, brings into question if this assay really was successful. However, RUNX1 is known to dimerise with itself as part of its normal function (Li *et al.* 2007). Therefore, the abundance of RUNX1 measured in this experiment may specifically have been the outcome of increased RUNX1 homodimerisation. Therefore, in conclusion, despite this limitation, there is precedent for the use of such a PLA flow cytometry protocol to assess the aptamer-induced modulation of HIF-1α:cofactor complexes, as we have shown here, when such anti-HIF aptamers become available. Such experimentation however, was beyond the scope of this study.

5.Conclusions

To conclude: JAK2VF and TPO inhibit the formation of HIF-1α:NPM1 complexes in Ba/F3-hMPL cells by a mechanism that is yet to be elucidated, supporting the hypothesis that oncogenic JAK2F signalling may induce phosphorylation of HIF-1α, and modulate its interaction with NPM1, but leaving open the potential role of ERK1/2 and HIF-1α in this JAK2VF context. This suggests a role for HIF-1α-cofactor interactions as mediators of downstream JAK2VF effects; by bioinformatic analysis, and immunoprecipitation of HIF-1α, HSPA2 has been highlighted as a potential onco-specific cofactor in JAK2VF-driven haematological malignancy, supporting the hypothesis that there are onco-specific HIF-1α interactors in a JAK2VF context. Lastly a commercially available aptamer was shown to target phospho-ERK, a mediator of HIF:cofactor interaction (Koukoulas *et al.*, 2021) in the nuclei of live cells in response to TPO signalling, but did not affect the phosphorylation status of either ERK1/2 or HIF-1α. The present work did not demonstrate the mechanism by which the complexes of HSPA2 and NPM1 with HIF-1α were modulated by JAK2VF or TPO-induced signalling. Given both are contexts in which HIF-1α is stabilised as a result of reactive oxygen species (ROS) (Yoshida *et al.*, 2008; Baumeister *et al.*, 2020), future work may benefit from assessment of the role of ROS in HIF-1α:cofactor interactions, in tandem with investigation of the potential modulatory role of non-ERK effectors of JAK2VF such as STATs (Wolf *et al.*, 2013; Hu *et al.*, 2022), which were not explored here. Within this project, the exploration of the therapeutic potential of aptamers with regard to HIF complexes was limited by the unavailability of aptamers that target HIFs. Future studies

using commercially available aptamers may be better suited to investigating aptamers' ability to interrupt endogenous protein interactions, which has been suggested as a mechanism of action for aptamer therapy (Lee *et al.*, 2005); for example ERK1/2 is dephosphorylated at a threonine and tyrosine phospho-site by physical interaction with DUSP6 (Arkell *et al.*, 2008). Hence, studying whether a phospho-ERK1 targeted aptamer, such as the one utilised in this project, might modulate such an interaction could still inform on the ability of these oligonucleotides to modulate intracellular protein interactions, as proof of principle - in lieu of anti-HIF aptamers. However, direct testing of the hypothesis that aptamers might modulate HIF complexes was beyond the scope of this project.

6.References

Adelman, D.M., Maltepe, E. and Simon, M.C. (1999) 'Multilineage embryonic hematopoiesis requires hypoxic ARNT activity', *Genes & development*, 13(19), pp. 2478–2483.

Akashi, K. *et al*. (2000) 'A clonogenic common myeloid progenitor that gives rise to all myeloid lineages', *Nature*, 404(6774), pp. 193–197.

Almedal, H. *et al.* (2016) 'Myeloproliferative neoplasms and JAK2 mutations', *Tidsskrift for den Norske laegeforening: tidsskrift for praktisk medicin, ny raekke*, 136(22), pp. 1889–1894.

Appelhoff, R.J. *et al.* (2004) 'Differential function of the prolyl hydroxylases PHD1, PHD2, and PHD3 in the regulation of hypoxia-inducible factor', *The Journal of biological chemistry*, 279(37), pp. 38458–38465.

Arkell, R.S. *et al.* (2008) 'DUSP6/MKP-3 inactivates ERK1/2 but fails to bind and inactivate ERK5', *Cellular signalling*, 20(5), pp. 836–843.

Automate stack splitter frame numbers (2020) *Image.sc Forum*. Available at: https://forum.image.sc/t/automate-stack-splitter-frame-numbers/36700 (Accessed: 30 January 2023).

Aynardi, J. *et al.* (2018) 'JAK2 V617F-positive acute myeloid leukaemia (AML): a comparison between de novo AML and secondary AML transformed from an underlying myeloproliferative neoplasm. A study from the Bone Marrow Pathology Group', *British journal of haematology*, 182(1), pp. 78–85.

Baldridge, M.T. *et al*. (2010) 'Quiescent haematopoietic stem cells are activated by IFN-gamma in response to chronic infection', *Nature*, 465(7299), pp. 793–797.

Barrio, S. *et al.* (2013) 'Inhibition of related JAK/STAT pathways with molecular targeted drugs shows strong synergy with ruxolitinib in chronic myeloproliferative neoplasm', *British journal of haematology*, 161(5), pp. 667–676.

Basu, M. *et al*. (2021) 'High nuclear expression of HIF1α, synergizing with inactivation of LIMD1 and VHL, portray worst prognosis among the bladder cancer patients: association with arsenic prevalence', *Journal of cancer research and clinical oncology*, 147(8), pp. 2309–2322.

Baumeister, J. *et al.* (2020) 'Hypoxia-inducible factor 1 (HIF-1) is a new therapeutic target in JAK2V617F-positive myeloproliferative neoplasms', *Leukemia*, 34(4), pp. 1062–1074.

Benito, J. *et al.* (2011) 'Pronounced hypoxia in models of murine and human leukemia: high efficacy of hypoxia-activated prodrug PR-104', *PloS one*, 6(8), p. e23108.

Berra, E. *et al.* (2003) 'HIF prolyl-hydroxylase 2 is the key oxygen sensor setting low steady-state levels of HIF-1alpha in normoxia', *The EMBO journal*, 22(16), pp. 4082–4090.

Bernitz, J.M. *et al*. (2016) 'Hematopoietic Stem Cells Count and Remember Self-Renewal Divisions', *Cell*, 167(5), pp. 1296–1309.e10.

Bonagura, T.W. *et al*. (2022) 'Quantification of Protein Expression by Proximity Ligation Assay in the Nonhuman Primate in Response to Estrogen', in K.M. Eyster (ed.) Estrogen *Receptors: Methods and Protocols*. New York, NY: Springer US, pp. 77–93.

Brkic, S. *et al.* (2021) 'Dual targeting of JAK2 and ERK interferes with the myeloproliferative neoplasm clone and enhances therapeutic efficacy', *Leukemia*, 35(10), pp. 2875–2884.

Bromfield, E.G. *et al*. (2017) 'Proteolytic degradation of heat shock protein A2 occurs in response to oxidative stress in male germ cells of the mouse', *Molecular human reproduction*, 23(2), pp. 91–105.

de Bruijn, M.F. *et al*. (2000) 'Definitive hematopoietic stem cells first develop within the major arterial regions of the mouse embryo', *The EMBO journal*, 19(11), pp. 2465–2474.

De Bruijn, M.F.T.R. *et al*. (2002) 'Hematopoietic stem cells localize to the endothelial cell layer in the midgestation mouse aorta', *Immunity*, 16(5), pp. 673–683.

Brunetti, L. *et al*. (2018) 'Mutant NPM1 Maintains the Leukemic State through HOX Expression', *Cancer cell*, 34(3), pp. 499–512.e9.

Bryce Drylie, Cathy Hawley, Ruth Ellerington (2022) 'unpublished data: 2 biological replicates of a phosho-flow assay to determine the effect of U0126, Ruxolitinib, and anti-phospho-ERK1 aptamer upon ERK1/2 and HIF-1alpha phosphorylation'.

Calvi, L.M. *et al*. (2003) 'Osteoblastic cells regulate the haematopoietic stem cell niche', *Nature*, 425(6960), pp. 841–846.

Cao, L. *et al*. (2019) 'Downregulation of HSPA2 inhibits proliferation via ERK1/2 pathway and endoplasmic reticular stress in lung adenocarcinoma'*, Annals of translational medicine*, 7(20), p. 540.

Casillas, A.L. *et al.* (2021) 'Direct phosphorylation and stabilization of HIF-1α by PIM1 kinase drives angiogenesis in solid tumors', *Oncogene*, 40(32), pp. 5142–5152.

Catarzi, S. *et al.* (2011) 'Redox regulation of ERK1/2 activation induced by sphingosine 1-phosphate in fibroblasts: involvement of NADPH oxidase and platelet-derived growth factor receptor', *Biochimica et biophysica acta*, 1810(4), pp. 446–456.

Center for Drug Evaluation and Research (no date) *FDA approves drug for adults with rare form of bone marrow disorder*, *U.S. Food and Drug Administration*. FDA. Available at: https://www.fda.gov/drugs/news-events-human-drugs/fda-approves-drug-adults-rare-form-bone-marrow-disorder (Accessed: 26 January 2023).

Cerami, E. *et al.* (2012) 'The cBio cancer genomics portal: an open platform for exploring multidimensional cancer genomics data', *Cancer discovery*, 2(5), pp. 401–404.

Cheloni, G. *et al.* (2017) 'Targeting chronic myeloid leukemia stem cells with the hypoxia-

inducible factor inhibitor acriflavine', *Blood*, 130(5), pp. 655–665.

Chen, M.J. *et al*. (2009) 'Runx1 is required for the endothelial to haematopoietic cell transition but not thereafter', *Nature*, 457(7231), pp. 887–891.

Chen, R.H., Sarnecki, C. and Blenis, J. (1992) 'Nuclear localization and regulation of erk- and rsk-encoded protein kinases', *Molecular and cellular biology*, 12(3), pp. 915–927.

Chou, F.-S. *et al*. (2012) 'The thrombopoietin/MPL/Bcl-xL pathway is essential for survival and self-renewal in human preleukemia induced by AML1-ETO', *Blood*, 120(4), pp. 709–719.

Christensen, J.L. and Weissman, I.L. (2001) 'Flk-2 is a marker in hematopoietic stem cell differentiation: a simple method to isolate long-term stem cells', *Proceedings of the National Academy of Sciences of the United States of America*, 98(25), pp. 14541–14546.

Coltella, N. *et al.* (2015) 'Synergistic Leukemia Eradication by Combined Treatment with Retinoic Acid and HIF Inhibition by EZN-2208 (PEG-SN38) in Preclinical Models of PML-RARα and PLZF-RARα-Driven Leukemia', *Clinical cancer research: an official journal of the American Association for Cancer Research*, 21(16), pp. 3685–3694.

Comazzetto, S. *et al*. (2019) 'Restricted Hematopoietic Progenitors and Erythropoiesis Require SCF from Leptin Receptor+ Niche Cells in the Bone Marrow', *Cell stem cell*, 24(3), pp. 477–486.e6.

Cumano, A. *et al*. (2001) 'Intraembryonic, but not yolk sac hematopoietic precursors, isolated before circulation, provide long-term multilineage reconstitution'*, Immunity*, 15(3), pp. 477–485.

David Kealy (2021) 'unpublished data: HIF-1alpha RIME carried out upon serum and cytokine starved hMPL-expressing UT7s expressing JAK2V617F or WT JAK2 in hypoxia, normoxia, 100ng ml^-1 TPO overnight'.

Deeb, G. *et al.* (2011) 'Hypoxia-inducible factor-1α protein expression is associated with poor survival in normal karyotype adult acute myeloid leukemia', *Leukemia research*, 35(5), pp. 579–584.

Depping, R. *et al*. (2019) 'The Nuclear Export Inhibitor Selinexor Inhibits Hypoxia Signaling Pathways And 3D Spheroid Growth Of Cancer Cells', *OncoTargets* and therapy, 12, pp. 8387–8399.

Desplat, V. *et al.* (2002) 'Hypoxia modifies proliferation and differentiation of CD34(+) CML cells', *Stem cells*, 20(4), pp. 347–354.

Drolet, D.W. *et al.* (2000) 'Pharmacokinetics and safety of an anti-vascular endothelial growth factor aptamer (NX1838) following injection into the vitreous humor of rhesus monkeys', *Pharmaceutical research*, 17(12), pp. 1503–1510.

Drolle, H. *et al.* (2015) 'Hypoxia regulates proliferation of acute myeloid leukemia and sensitivity against chemotherapy', *Leukemia research*, 39(7), pp. 779–785.

Dutta, A., Hutchison, R.E. and Mohi, G. (2017) 'Hmga2 promotes the development of myelofibrosis in Jak2V617F knockin mice by enhancing TGF-β1 and Cxcl12 pathways', *Blood*, 130(7), pp. 920–932.

Eliasson, P. *et al.* (2010) 'Hypoxia mediates low cell-cycle activity and increases the proportion of long-term-reconstituting hematopoietic stem cells during in vitro culture', *Experimental hematology*, 38(4), pp. 301–310.e2.

Eric Huang, L. *et al.* (1996) 'Activation of Hypoxia-inducible Transcription Factor Depends

Primarily upon Redox-sensitive Stabilization of Its α Subunit *', *The Journal of biological chemistry*, 271(50), pp. 32253–32259.

Falini, B. *et al.* (2005) 'Cytoplasmic nucleophosmin in acute myelogenous leukemia with a normal karyotype', *The New England journal of medicine*, 352(3), pp. 254–266.

Falini, B. *et al.* (2006) 'Both carboxy-terminus NES motif and mutated tryptophan(s) are crucial for aberrant nuclear export of nucleophosmin leukemic mutants in NPMc+ AML', *Blood*, 107(11), pp. 4514–4523.

Fiskus, W. *et al.* (2011) 'Heat shock protein 90 inhibitor is synergistic with JAK2 inhibitor and overcomes resistance to JAK2-TKI in human myeloproliferative neoplasm cells', *Clinical cancer research: an official journal of the American Association for Cancer Research*, 17(23), pp. 7347–7358.

FlowJo™ Software - for Windows (no date). Ashland, OR: Becton, Dickinson and Company; 2021.

Forthun, R.B. *et al.* (2012) 'Cross-species functional genomic analysis identifies resistance genes of the histone deacetylase inhibitor valproic acid', *PloS one*, 7(11), p. e48992.

Foxler, D.E. *et al.* (2012) 'The LIMD1 protein bridges an association between the prolyl hydroxylases and VHL to repress HIF-1 activity', *Nature cell biology*, 14(2), pp. 201–208.

Gao, J. *et al.* (2013) 'Integrative analysis of complex cancer genomics and clinical profiles using the cBioPortal', *Science signaling*, 6(269), p. l1.

Garg, M. *et al.* (2010) 'Heat-shock protein 70-2 (HSP70-2) expression in bladder urothelial carcinoma is associated with tumour progression and promotes migration and invasion', *European journal of cancer*, 46(1), pp. 207–215.

Gaur, M. *et al.* (2001) 'Characterization of Mpl mutants using primary megakaryocyte-lineage cells from mpl−/−mice: a new system for Mpl structure–function studies', *Blood*, 97(6), pp. 1653–1661.

Ganuza, M. *et al*. (2018) 'Murine hematopoietic stem cell activity is derived from pre-circulation embryos but not yolk sacs', *Nature communications*, 9(1), p. 5405.

Gekas, C. *et al*. (2005) 'The placenta is a niche for hematopoietic stem cells', *Developmental cell*, 8(3), pp. 365–375.

Giuntoli, S. *et al.* (2007) 'Severe hypoxia defines heterogeneity and selects highly immature progenitors within clonal erythroleukemia cells', *Stem cells*, 25(5), pp. 1119–1125.

Giuntoli, S. *et al.* (2011) 'Glucose availability in hypoxia regulates the selection of chronic myeloid leukemia progenitor subsets with different resistance to imatinib-mesylate', *Haematologica*, 96(2), pp. 204–212.

Goedhart, J. (2019) *Data manipulation? It's normal(ization)!* Available at: https://thenode.biologists.com/data-normalization/research/ (Accessed: 29 January 2023).

Gordon-Keylock, S. *et al*. (2013) 'Mouse extraembryonic arterial vessels harbor precursors capable of maturing into definitive HSCs', *Blood*, 122(14), pp. 2338–2345.

Gómez-Torres, M.J. *et al.* (2022) 'Molecular Chaperone HSPA2 Distribution During Hyaluronic Acid Selection in Human Sperm', *Reproductive sciences* [Preprint]. Available at: https://doi.org/10.1007/s43032-022-01031-9.

Gray, M.J. *et al.* (2005) 'HIF-1alpha, STAT3, CBP/p300 and Ref-1/APE are components of a transcriptional complex that regulates Src-dependent hypoxia-induced expression of

VEGF in pancreatic and prostate carcinomas', *Oncogene*, 24(19), pp. 3110–3120.

Greenbaum, A. *et al*. (2013) 'CXCL12 in early mesenchymal progenitors is required for haematopoietic stem-cell maintenance', *Nature*, 495(7440), pp. 227–230.

Grisouard, J. *et al*. (2015) 'Deletion of Stat3 in hematopoietic cells enhances thrombocytosis and shortens survival in a JAK2-V617F mouse model of MPN', *Blood*, 125(13), pp. 2131–2140.

Habryka, A. *et al.* (2015) 'Cell type-dependent modulation of the gene encoding heat shock protein HSPA2 by hypoxia-inducible factor HIF-1: Down-regulation in keratinocytes and up-regulation in HeLa cells', *Biochimica et biophysica acta*, 1849(9), pp. 1155–1169.

Halvarsson, C. *et al.* (2019) 'Putative Role of Nuclear Factor-Kappa B But Not Hypoxia-Inducible Factor-1α in Hypoxia-Dependent Regulation of Oxidative Stress in Hematopoietic Stem and Progenitor Cells', *Antioxidants & redox signaling*, 31(3), pp. 211–226.

Hammoud, M. *et al.* (2012) 'Combination of low O(2) concentration and mesenchymal stromal cells during culture of cord blood CD34(+) cells improves the maintenance and proliferative capacity of hematopoietic stem cells', *Journal of cellular physiology*, 227(6), pp. 2750–2758.

Hayashi, Y. *et al.* (2018) 'Pathobiological Pseudohypoxia as a Putative Mechanism Underlying Myelodysplastic Syndromes', *Cancer discovery*, 8(11), pp. 1438–1457.

Henry, L. and Wickham, H. (2020) 'Purrr: Functional programming tools'.

Hermitte, F. *et al.* (2006) 'Very low O2 concentration (0.1%) favors G0 return of dividing CD34+ cells', *Stem cells*, 24(1), pp. 65–73.

Hewitson, K.S. *et al.* (2002) 'Hypoxia-inducible factor (HIF) asparagine hydroxylase is identical to factor inhibiting HIF (FIH) and is related to the cupin structural family', *The Journal of biological chemistry*, 277(29), pp. 26351–26355.

Hirsilä, M. *et al.* (2003) 'Characterization of the Human Prolyl 4-Hydroxylases That Modify the Hypoxia-inducible Factor*', *The Journal of biological chemistry*, 278(33), pp. 30772–30780.

HSPA1A heat shock protein family A (Hsp70) member 1A [Homo sapiens (human)] (14-Jan-2023) *National Center for Biotechnology Information (NCBI)[Internet]. Bethesda (MD): National Library of Medicine (US), National Center for Biotechnology Information*. Available at: https://www.ncbi.nlm.nih.gov/gene/3303 (Accessed: 19-Jan-2023).

Huang, W.-J. *et al.* (2009) 'Transcriptional upregulation of HSP70-2 by HIF-1 in cancer cells in response to hypoxia', *International journal of cancer. Journal international du cancer*, 124(2), pp. 298–305.

Hu, M. *et al.* (2022) 'Preclinical studies of Flonoltinib Maleate, a novel JAK2/FLT3 inhibitor, in treatment of JAK2V617F-induced myeloproliferative neoplasms', *Blood cancer journal*, 12(3), p. 37.

imagej.nih.gov (2018). Available at: https://imagej.nih.gov/ij/developer/macro/functions.html (Accessed: 29 January 2023).

Itkin, T. *et al.* (2016) 'Distinct bone marrow blood vessels differentially regulate haematopoiesis', *Nature*, 532(7599), pp. 323–328.

Ivan, M. *et al.* (2001) 'HIFalpha targeted for VHL-mediated destruction by proline hydroxylation: implications for O2 sensing', *Science*, 292(5516), pp. 464–468.

Ivanović, Z. *et al.* (2000) 'Incubation of murine bone marrow cells in hypoxia ensures the maintenance of marrow-repopulating ability together with the expansion of committed progenitors', *British journal of haematology*, 108(2), pp. 424–429.

Ivanovic, Z. *et al.* (2002) 'Hypoxia maintains and interleukin-3 reduces the pre-colony-forming cell potential of dividing CD34(+) murine bone marrow cells', *Experimental hematology*, 30(1), pp. 67–73.

Ivanovic, Z. *et al.* (2004) 'Simultaneous maintenance of human cord blood SCID-repopulating cells and expansion of committed progenitors at low O2 concentration (3%)', *Stem cells*, 22(5), pp. 716–724.

Ivanovs, A. *et al*. (2011) 'Highly potent human hematopoietic stem cells first emerge in the intraembryonic aorta-gonad-mesonephros region', *The Journal of experimental medicine*, 208(12), pp. 2417–2427.

Ivanovs, A. *et al*. (2014) 'Identification of the niche and phenotype of the first human hematopoietic stem cells', *Stem cell reports*, 2(4), pp. 449–456.

Jaakkola, P. *et al.* (2001) 'Targeting of HIF-alpha to the von Hippel-Lindau ubiquitylation complex by O2-regulated prolyl hydroxylation', *Science*, 292(5516), pp. 468–472.

Jaenen, V. *et al.* (2021) 'Reactive oxygen species rescue regeneration after silencing the MAPK-ERK signaling pathway in Schmidtea mediterranea', *Scientific reports*, 11(1), p. 881.

Jakubison, B.L. *et al.* (2022) 'ID2 and HIF-1α collaborate to protect quiescent hematopoietic stem cells from activation, differentiation, and exhaustion', *The Journal of clinical investigation*, 132(13). Available at: https://doi.org/10.1172/JCI152599.

James, C. *et al.* (2005) 'A unique clonal JAK2 mutation leading to constitutive signalling causes polycythaemia vera', *Nature*, 434(7037), pp. 1144–1148.

Jiang, B.-H. *et al.* (1996) 'Dimerization, DNA Binding, and Transactivation Properties of Hypoxia-inducible Factor 1 *', *The Journal of biological chemistry*, 271(30), pp. 17771–17778.

Jordan, C.T. and Lemischka, I.R. (1990) 'Clonal and systemic analysis of long-term hematopoiesis in the mouse'*, Genes & development*, 4(2), pp. 220–232.

Jozwik, K.M. *et al.* (2016) 'FOXA1 Directs H3K4 Monomethylation at Enhancers via Recruitment of the Methyltransferase MLL3', *Cell reports*, 17(10), pp. 2715–2723.

Jung, J.E. *et al*. (2008) 'STAT3 inhibits the degradation of HIF-1alpha by pVHL-mediated ubiquitination', *Experimental & molecular medicine*, 40(5), pp. 479–485.

Kallio, P.J. *et al.* (1999) 'Regulation of the Hypoxia-inducible Transcription Factor 1α by the Ubiquitin-Proteasome Pathway *', *The Journal of biological chemistry*, 274(10), pp. 6519–6525.

Kassambara, A. (2020) 'rstatix: Pipe-friendly framework for basic statistical tests'.

Kelley, J.B. and Paschal, B.M. (2019) 'Fluorescence-based quantification of nucleocytoplasmic transport', *Methods* , 157, pp. 106–114.

Khan, I. *et al.* (2013) 'AKT is a therapeutic target in myeloproliferative neoplasms', *Leukemia*, 27(9), pp. 1882–1890.

Kim, K. *et al.* (2014) 'Efficient isolation and elution of cellular proteins using aptamer-mediated protein precipitation assay', *Biochemical and biophysical research communications*, 448(1), pp. 114–119.

Kiel, M.J. *et al*. (2005) ‘SLAM family receptors distinguish hematopoietic stem and progenitor cells and reveal endothelial niches for stem cells’, *Cell*, 121(7), pp. 1109–1121.

Kiss, S. *et al.* (2018) ‘Endophthalmitis rates among patients receiving intravitreal anti-VEGF injections: a USA claims analysis’, *Clinical ophthalmology* , 12, pp. 1625–1635.

Kissa, K. and Herbomel, P. (2010) ‘Blood stem cells emerge from aortic endothelium by a novel type of cell transition’, *Nature*, 464(7285), pp. 112–115.

Klimczak, M. *et al.* (2019) ‘Heat shock proteins create a signature to predict the clinical outcome in breast cancer’, *Scientific reports*, 9(1), p. 7507.

Kondo, M., Weissman, I.L. and Akashi, K. (1997) ‘Identification of clonogenic common lymphoid progenitors in mouse bone marrow’, *Cell*, 91(5), pp. 661–672.

Koukoulas, K. *et al.* (2021) ‘ERK signaling controls productive HIF-1 binding to chromatin and cancer cell adaptation to hypoxia through HIF-1α interaction with NPM1’, *Molecular oncology*, 15(12), pp. 3468–3489.

Kourti, M. *et al.* (2015) ‘CK1δ restrains lipin-1 induction, lipid droplet formation and cell proliferation under hypoxia by reducing HIF-1α/ARNT complex formation’, *Cellular signalling*, 27(6), pp. 1129–1140.

Kovacević-Filipović, M. *et al.* (2007) ‘Interleukin-6 (IL-6) and low O(2) concentration (1%) synergize to improve the maintenance of hematopoietic stem cells (pre-CFC)’, *Journal of cellular physiology*, 212(1), pp. 68–75.

Kralovics, R. *et al.* (2005) ‘A gain-of-function mutation of JAK2 in myeloproliferative disorders’, *The New England journal of medicine*, 352(17), pp. 1779–1790.

Kratschmer, C. and Levy, M. (2017) ‘Effect of Chemical Modifications on Aptamer Stability in Serum’, *Nucleic acid therapeutics*, 27(6), pp. 335–344.

Kubota, Y., Takubo, K. and Suda, T. (2008) ‘Bone marrow long label-retaining cells reside in the sinusoidal hypoxic niche’, *Biochemical and biophysical research communications*, 366(2), pp. 335–339.

Kunisaki, Y. *et al*. (2013) ‘Arteriolar niches maintain haematopoietic stem cell quiescence’, *Nature*, 502(7473), pp. 637–643.

Lando, D. *et al.* (2002) ‘Asparagine hydroxylation of the HIF transactivation domain a hypoxic switch’, *Science*, 295(5556), pp. 858–861.

Lee, J.-H. *et al.* (2005) ‘A therapeutic aptamer inhibits angiogenesis by specifically targeting the heparin binding domain of VEGF165’, *Proceedings of the National Academy of Sciences of the United States of America*, 102(52), pp. 18902–18907.

Levine, R.L. *et al.* (2005) ‘The JAK2V617F activating mutation occurs in chronic myelomonocytic leukemia and acute myeloid leukemia, but not in acute lymphoblastic leukemia or chronic lymphocytic leukemia’, *Blood*, 106(10), pp. 3377–3379.

Li, D. *et al*. (2007) ‘RUNX1-RUNX1 homodimerization modulates RUNX1 activity and function’, *The Journal of biological chemistry*, 282(18), pp. 13542–13551.

Li, H.-S. *et al*. (2019) ‘HIF-1α protects against oxidative stress by directly targeting mitochondria’, *Redox biology*, 25, p. 101109.

Li, R. *et al*. (2020) ‘JAK2V617F Mutation Promoted IL-6 Production and Glycolysis via Mediating PKM1 Stabilization in Macrophages’, *Frontiers in immunology*, 11, p. 589048.

Liu, K.-H. *et al*. (2018) ‘Hypoxia Stimulates the Epithelial-to-Mesenchymal Transition in

Lung Cancer Cells Through Accumulation of Nuclear β-Catenin', *Anticancer research*, 38(11), pp. 6299–6308.

Lo Celso, C. *et al.* (2009) 'Live-animal tracking of individual haematopoietic stem/progenitor cells in their niche', *Nature*, 457(7225), pp. 92–96.

Luo, W. *et al.* (2010) 'Hsp70 and CHIP selectively mediate ubiquitination and degradation of hypoxia-inducible factor (HIF)-1alpha but Not HIF-2alpha', *The Journal of biological chemistry*, 285(6), pp. 3651–3663.

Machlus, K.R. *et al*. (2017) 'Selinexor-induced thrombocytopenia results from inhibition of thrombopoietin signaling in early megakaryopoiesis', *Blood*, 130(9), pp. 1132–1143.

Marty, C. *et al*. (2013) 'A role for reactive oxygen species in JAK2 V617F myeloproliferative neoplasm progression', *Leukemia*, 27(11), pp. 2187–2195.

Marubayashi, S. *et al.* (2010) 'HSP90 is a therapeutic target in JAK2-dependent myeloproliferative neoplasms in mice and humans', *The Journal of clinical investigation*, 120(10), pp. 3578–3593.

Masson, N. *et al.* (2001) 'Independent function of two destruction domains in hypoxia-inducible factor-alpha chains activated by prolyl hydroxylation', *The EMBO journal*, 20(18), pp. 5197–5206.

Matsunaga, T. *et al.* (2012) 'Elevated HIF-1α expression of acute myelogenous leukemia stem cells in the endosteal hypoxic zone may be a cause of minimal residual disease in bone marrow after chemotherapy', *Leukemia research*, 36(6), pp. e122–4.

McKeown, S.R. (2014) 'Defining normoxia, physoxia and hypoxia in tumours-implications for treatment response', *The British journal of radiology*, 87(1035), p. 20130676.

McKerrell, T. *et al.* (2017) 'JAK2 V617F hematopoietic clones are present several years prior to MPN diagnosis and follow different expansion kinetics', *Blood advances*, 1(14), pp. 968–971.

Medvinsky, A. and Dzierzak, E. (1996) 'Definitive hematopoiesis is autonomously initiated by the AGM region', *Cell*, 86(6), pp. 897–906.

Metzen, E. *et al.* (2005) 'Regulation of the prolyl hydroxylase domain protein 2 (phd2/egln-1) gene: identification of a functional hypoxia-responsive element', *Biochemical Journal*, 387(Pt 3), pp. 711–717.

Microsoft (2011) *Microsoft Excel* [Windows]. Available at: https://www.microsoft.com/en-gb/microsoft-365/business/compare-all-microsoft-365-business-products-b?&ef_id=Cj0KCQiAz9ieBhCIARIsACB0oGKMHy-U85keLZftg2xpmEqEj5L9CJ25jMcc1dcrDmdrb7kpkaFACWIaAjXeEALw_wcB:G:s&OCID=AIDcmmwf9kwzdj_SEM_Cj0KCQiAz9ieBhCIARIsACB0oGKMHy-U85keLZftg2xpmEqEj5L9CJ25jMcc1dcrDmdrb7kpkaFACWIaAjXeEALw_wcB:G:s&lnkd=Google_O365SMB_Brand&gclid=Cj0KCQiAz9ieBhCIARIsACB0oGKMHy-U85keLZftg2xpmEqEj5L9CJ25jMcc1dcrDmdrb7kpkaFACWIaAjXeEALw_wcB.

Minet, E. *et al.* (1999) 'Hypoxia-induced activation of HIF-1: role of HIF-1alpha-Hsp90 interaction', *FEBS letters*, 460(2), pp. 251–256.

Mohammed, H. *et al.* (2013) 'Endogenous purification reveals GREB1 as a key estrogen receptor regulatory factor', *Cell reports*, 3(2), pp. 342–349.

Mohammed, H. *et al.* (2015) 'Progesterone receptor modulates ERα action in breast cancer', *Nature*, 523(7560), pp. 313–317.

Mo, J.-H. *et al.* (2012) 'HIF-1α and HSP90: target molecules selected from a tumorigenic papillary thyroid carcinoma cell line', *Cancer science*, 103(3), pp. 464–471.

Montalban-Bravo, G. *et al.* (2019) 'NPM1 mutations define a specific subgroup of MDS and MDS/MPN patients with favorable outcomes with intensive chemotherapy', *Blood advances*, 3(6), pp. 922–933.

Mossadegh-Keller, N. *et al*. (2013) 'M-CSF instructs myeloid lineage fate in single haematopoietic stem cells', *Nature*, 497(7448), pp. 239–243.

Ng, E.W.M. *et al.* (2006) 'Pegaptanib, a targeted anti-VEGF aptamer for ocular vascular disease', *Nature reviews. Drug discovery*, 5(2), pp. 123–132.

Oku, S. *et al*. (2010) 'JAK2 V617F uses distinct signalling pathways to induce cell proliferation and neutrophil activation', *British journal of haematology*, 150(3), pp. 334–344.

Ong, Q. *et al.* (2015) 'U0126 protects cells against oxidative stress independent of its function as a MEK inhibitor', *ACS chemical neuroscience*, 6(1), pp. 130–137.

Osawa, M. *et al*. (1996) 'Long-term lymphohematopoietic reconstitution by a single CD34-low/negative hematopoietic stem cell', *Science*, 273(5272), pp. 242–245.

Parmar, K. *et al.* (2007) 'Distribution of hematopoietic stem cells in the bone marrow according to regional hypoxia', *Proceedings of the National Academy of Sciences of the United States of America*, 104(13), pp. 5431–5436.

Pasqualucci, L. *et al.* (2008) 'NPM1-mutated acute myeloid leukaemia occurring in JAK2-V617F+ primary myelofibrosis: de-novo origin?', *Leukemia*, 22(7), pp. 1459–1463.

Pedersen, M. *et al.* (2008) 'Stem cell factor induces HIF-1alpha at normoxia in hematopoietic cells', *Biochemical and biophysical research communications*, 377(1), pp. 98–103.

Perlson, E. *et al.* (2006) 'Vimentin binding to phosphorylated Erk sterically hinders enzymatic dephosphorylation of the kinase', *Journal of molecular biology*, 364(5), pp. 938–944.

Pianigiani, G. *et al*. (2022) 'Prolonged XPO1 inhibition is essential for optimal antileukemic activity in NPM1-mutated AML', *Blood advances*, 6(22), pp. 5938–5949.

Pietras, E.M. *et al*. (2016) 'Chronic interleukin-1 exposure drives haematopoietic stem cells towards precocious myeloid differentiation at the expense of self-renewal', *Nature* cell biology, 18(6), pp. 607–618.

Piccoli, C. *et al.* (2007) 'The hypoxia-inducible factor is stabilized in circulating hematopoietic stem cells under normoxic conditions', *FEBS letters*, 581(16), pp. 3111–3119.

Pugh, C.W. *et al.* (1997) 'Activation of Hypoxia-inducible Factor-1; Definition of Regulatory Domains within the α Subunit *', *The Journal of biological chemistry*, 272(17), pp. 11205–11214.

Pulikkan, J.A. *et al*. (2012) 'Thrombopoietin/MPL participates in initiating and maintaining RUNX1-ETO acute myeloid leukemia via PI3K/AKT signaling', *Blood*, 120(4), pp. 868–879.

Raedler, L.A. (2015) 'Jakafi (Ruxolitinib): First FDA-Approved Medication for the Treatment of Patients with Polycythemia Vera', *American health & drug benefits*, 8(Spec Feature), pp. 75–79.

Rao, T.N. *et al*. (2021) 'JAK2-V617F and interferon-α induce megakaryocyte-biased stem cells characterized by decreased long-term functionality', *Blood*, 137(16), pp. 2139–2151.

R Core Team (2021) *R: A Language and Environment for Statistical Computing*. Vienna, Austria: R Foundation for Statistical Computing. Available at: https://www.R-project.org/.

Redgrove, K.A. *et al.* (2012) 'The molecular chaperone HSPA2 plays a key role in regulating the expression of sperm surface receptors that mediate sperm-egg recognition', *PloS one*, 7(11), p. e50851.

Reyes-Reyes, E.M., Teng, Y. and Bates, P.J. (2010) 'A new paradigm for aptamer therapeutic AS1411 action: uptake by macropinocytosis and its stimulation by a nucleolin-dependent mechanism', *Cancer research*, 70(21), pp. 8617–8629.

Richard, D.E. *et al.* (1999) 'p42/p44 Mitogen-activated Protein Kinases Phosphorylate Hypoxia-inducible Factor 1α (HIF-1α) and Enhance the Transcriptional Activity of HIF-1 *', *The Journal of biological chemistry*, 274(46), pp. 32631–32637.

Rojnuckarin, P., Drachman, J.G. and Kaushansky, K. (1999) 'Thrombopoietin-induced activation of the mitogen-activated protein kinase (MAPK) pathway in normal megakaryocytes: role in endomitosis', *Blood*, 94(4), pp. 1273–1282.

Romain Guiet (no date) *An imagej macro example to process a folder of images, split the channels and save them in an output directory*. Github. Available at: https://gist.github.com/romainGuiet/cf42f3b1d31222a76d602dfe2f028894 (Accessed: 30 January 2023).

RStudio Team (2016) *RStudio: Integrated Development Environment for R*. Boston, MA: RStudio, Inc. Available at: http://www.rstudio.com/.

Salceda, S. and Caro, J. (1997) 'Hypoxia-inducible Factor 1α (HIF-1α) Protein Is Rapidly Degraded by the Ubiquitin-Proteasome System under Normoxic Conditions: ITS STABILIZATION BY HYPOXIA DEPENDS ON REDOX-INDUCED CHANGES*', *The Journal of biological chemistry*, 272(36), pp. 22642–22647.

Sangkhae, V., Saur, S.J., *et al.* (2014) 'Phosphorylated c-Mpl tyrosine 591 regulates thrombopoietin-induced signaling', *Experimental hematology*, 42(6), pp. 477–86.e4.

Sangkhae, V., Etheridge, S.L., *et al.* (2014) 'The thrombopoietin receptor, MPL, is critical for development of a JAK2V617F-induced myeloproliferative neoplasm', *Blood*, 124(26), pp. 3956–3963.

Sawai, C.M. *et al*. (2016) 'Hematopoietic Stem Cells Are the Major Source of Multilineage Hematopoiesis in Adult Animals', *Immunity*, 45(3), pp. 597–609.

Schindelin, J. *et al.* (2012) 'Fiji: an open-source platform for biological-image analysis', *Nature methods*, 9(7), pp. 676–682.

Semenza, G.L. *et al.* (1991) 'Hypoxia-inducible nuclear factors bind to an enhancer element located 3' to the human erythropoietin gene', *Proceedings of the National Academy of Sciences of the United States of America*, 88(13), pp. 5680–5684.

Semenza, G.L. and Wang, G.L. (1992) 'A nuclear factor induced by hypoxia via de novo protein synthesis binds to the human erythropoietin gene enhancer at a site required for transcriptional activation', *Molecular and cellular biology*, 12(12), pp. 5447–5454.

Shentu, Y. *et al.* (2020) 'Nestin Promotes Peritoneal Fibrosis by Protecting HIF1-α From Proteasomal Degradation', *Frontiers in physiology*, 11, p. 517912.

Shih, J.-W. *et al.* (2017) 'Long noncoding RNA LncHIFCAR/MIR31HG is a HIF-1α co-

activator driving oral cancer progression', *Nature communications*, 8, p. 15874.

Shima, H. *et al.* (2009) 'Reconstitution activity of hypoxic cultured human cord blood CD34-positive cells in NOG mice', *Biochemical and biophysical research communications*, 378(3), pp. 467–472.

Singer, J.W. *et al.* (2016) 'Comprehensive kinase profile of pacritinib, a nonmyelosuppressive Janus kinase 2 inhibitor', *Journal of experimental pharmacology*, 8, pp. 11–19.

Slowikowski, K. (2021) *ggrepel: Automatically Position Non-Overlapping Text Labels with 'ggplot2'*. Available at: https://CRAN.R-project.org/package=ggrepel.

Sojka, D.R. *et al.* (2020) 'HSPA2 Chaperone Contributes to the Maintenance of Epithelial Phenotype of Human Bronchial Epithelial Cells but Has Non-Essential Role in Supporting Malignant Features of Non-Small Cell Lung Carcinoma, MCF7, and HeLa Cancer Cells', *Cancers*, 12(10). Available at: https://doi.org/10.3390/cancers12102749.

Souied, E.H. *et al.* (2016) 'Severe Ocular Inflammation Following Ranibizumab or Aflibercept Injections for Age-Related Macular Degeneration: A Retrospective Claims Database Analysis', *Ophthalmic epidemiology*, 23(2), pp. 71–79.

Spangrude, G.J., Heimfeld, S. and Weissman, I.L. (1988) 'Purification and characterization of mouse hematopoietic stem cells', *Science*, 241(4861), pp. 58–62.

Spencer, J.A. *et al.* (2014) 'Direct measurement of local oxygen concentration in the bone marrow of live animals', *Nature*, 508(7495), pp. 269–273.

Stewart, E.R. *et al.* (2019) 'Maintenance of epigenetic landscape requires CIZ1 and is corrupted in differentiated fibroblasts in long-term culture', *Nature communications*, 10(1), p. 460.

Stivala, S. *et al.* (2019) 'Targeting compensatory MEK/ERK activation increases JAK inhibitor efficacy in myeloproliferative neoplasms', *The Journal of clinical investigation*, 129(4), pp. 1596–1611.

Takubo, K. *et al.* (2010) 'Regulation of the HIF-1alpha level is essential for hematopoietic stem cells', *Cell stem cell*, 7(3), pp. 391–402.

Tang, X. *et al.* (2021) 'Heat shock protein-90alpha (Hsp90α) stabilizes hypoxia-inducible factor-1α (HIF-1α) in support of spermatogenesis and tumorigenesis', *Cancer gene therapy*, 28(9), pp. 1058–1070.

Taoudi, S. and Medvinsky, A. (2007) 'Functional identification of the hematopoietic stem cell niche in the ventral domain of the embryonic dorsal aorta', *Proceedings of the National Academy of Sciences of the United States of America*, 104(22), pp. 9399–9403.

Tavian, M. *et al*. (2001) 'The human embryo, but not its yolk sac, generates lympho-myeloid stem cells: mapping multipotent hematopoietic cell fate in intraembryonic mesoderm', *Immunity*, 15(3), pp. 487–495.

Theodoropoulos, V.E. *et al*. (2004) 'Hypoxia-inducible factor 1 alpha expression correlates with angiogenesis and unfavorable prognosis in bladder cancer', *European urology*, 46(2), pp. 200–208.

Tong, H. *et al.* (2012) 'Hypoxia-inducible factor-1α expression indicates poor prognosis in myelodysplastic syndromes', *Leukemia & lymphoma*, 53(12), pp. 2412–2418.

Tuerk, C. and Gold, L. (1990) 'Systematic evolution of ligands by exponential enrichment: RNA ligands to bacteriophage T4 DNA polymerase', *Science*, 249(4968), pp. 505–510.

Tyner, J.W. *et al.* (2018) 'Functional genomic landscape of acute myeloid leukaemia', *Nature*, 562(7728), pp. 526–531.

US Department of Health and Human Services (23/March/2005) *Drug Approval Package Macugen (Pegaptanib Sodium) Injection*, *https://www.accessdata.fda.gov/*. Available at: https://www.accessdata.fda.gov/drugsatfda_docs/nda/2004/21-756_Macugen.cfm (Accessed: 26 January 2023).

Van Egeren, D. *et al.* (2021) 'Reconstructing the Lineage Histories and Differentiation Trajectories of Individual Cancer Cells in Myeloproliferative Neoplasms', *Cell stem cell*, 28(3), pp. 514–523.e9.

Velasco-Hernandez, T. *et al.* (2014) 'HIF-1α can act as a tumor suppressor gene in murine acute myeloid leukemia', *Blood*, 124(24), pp. 3597–3607.

Velasco-Hernandez, T. *et al.* (2019) 'Hif-1α Deletion May Lead to Adverse Treatment Effect in a Mouse Model of MLL-AF9-Driven AML', *Stem cell reports*, 12(1), pp. 112–121.

Verstovsek, S. *et al.* (2010) 'Safety and efficacy of INCB018424, a JAK1 and JAK2 inhibitor, in myelofibrosis', *The New England journal of medicine*, 363(12), pp. 1117–1127.

Verstovsek, S. *et al.* (2019) 'The Oral JAK2/IRAK1 Inhibitor Pacritinib Demonstrates Spleen Volume Reduction in Myelofibrosis Patients Independent of JAK2V617F Allele Burden', *Blood*, 134(Supplement_1), pp. 1674–1674.

Vukovic, M. *et al.* (2015) 'Hif-1α and Hif-2α synergize to suppress AML development but are dispensable for disease maintenance', *The Journal of experimental medicine*, 212(13), pp. 2223–2234.

Wang, G.L. and Semenza, G.L. (1993) 'General involvement of hypoxia-inducible factor 1 in transcriptional response to hypoxia', *Proceedings of the National Academy of Sciences of the United States of America*, 90(9), pp. 4304–4308.

Wang, M. *et al.* (2014) 'Mutation analysis of JAK2V617F, FLT3-ITD, NPM1, and DNMT3A in Chinese patients with myeloproliferative neoplasms', *BioMed research international*, 2014, p. 485645.

Wang, W. *et al*. (2010) 'AML1 is overexpressed in patients with myeloproliferative neoplasms and mediates JAK2V617F-independent overexpression of NF-E2', *Blood*, 116(2), pp. 254–266.

Wang, Y. *et al.* (2011) 'Targeting HIF1α eliminates cancer stem cells in hematological malignancies', *Cell stem cell*, 8(4), pp. 399–411.

Wang, Y. *et al.* (2014) 'Echinomycin protects mice against relapsed acute myeloid leukemia without adverse effect on hematopoietic stem cells', *Blood*, 124(7), pp. 1127–1135.

Wei, D. *et al*. (2013) 'Digoxin downregulates NDRG1 and VEGF through the inhibition of HIF-1α under hypoxic conditions in human lung adenocarcinoma A549 cells', *International journal of molecular sciences*, 14(4), pp. 7273–7285.

Wickham, H. *et al.* (no date) 'dplyr: A grammar of data manipulation', *R package version 0.4* [Preprint].

Wickham, H. and Bryan, J. (no date) 'readxl: Read excel files', *R package version* [Preprint].

Wickham, H. and Henry, L. (no date) 'Tidyr: Tidy messy data', *R package version* [Preprint].

Winkler, I.G. *et al.* (2010) 'Positioning of bone marrow hematopoietic and stromal cells relative to blood flow in vivo: serially reconstituting hematopoietic stem cells reside in distinct nonperfused niches', *Blood*, 116(3), pp. 375–385.

Wilson, A. *et al*. (2008) 'Hematopoietic stem cells reversibly switch from dormancy to self-renewal during homeostasis and repair', *Cell*, 135(6), pp. 1118–1129.

Wolf, A. *et al.* (2013) 'JAK2-V617F-induced MAPK activity is regulated by PI3K and acts synergistically with PI3K on the proliferation of JAK2-V617F-positive cells', *JAK-STAT*, 2(3), p. e24574.

Xie, Y. *et al.* (2009) 'Detection of functional haematopoietic stem cell niche using real-time imaging', *Nature*, 457(7225), pp. 97–101.

Xu, S. *et al*. (2021) 'IL-6 promotes nuclear translocation of HIF-1α to aggravate chemoresistance of ovarian cancer cells', *European journal of pharmacology*, 894, p. 173817.

Yan, D. *et al*. (2019) 'Nuclear-Cytoplasmic Transport Is a Therapeutic Target in Myelofibrosis', *Clinical cancer research: an official journal of the American Association for Cancer Research*, 25(7), pp. 2323–2335.

Yang, Y. *et al.* (2022) 'HIF-1 Interacts with TRIM28 and DNA-PK to release paused RNA polymerase II and activate target gene transcription in response to hypoxia', *Nature communications*, 13(1), p. 316.

Yoshida, K. *et al.* (2008) 'Thrombopoietin (TPO) regulates HIF-1alpha levels through generation of mitochondrial reactive oxygen species', *International journal of hematology*, 88(1), pp. 43–51.

Yoshihara, H. *et al*. (2007) 'Thrombopoietin/MPL signaling regulates hematopoietic stem cell quiescence and interaction with the osteoblastic niche', *Cell stem cell*, 1(6), pp. 685–697.

Yu, D. *et al.* (2013) 'Study of the selective uptake progress of aptamer-modified PLGA particles by liver cells', *Macromolecular bioscience*, 13(10), pp. 1413–1421.

Zhang, H. *et al.* (2012) 'HIF1α is required for survival maintenance of chronic myeloid leukemia stem cells', *Blood*, 119(11), pp. 2595–2607.

Zhang, H. *et al.* (2013) 'Overexpression of HSPA2 is correlated with poor prognosis in esophageal squamous cell carcinoma', *World journal of surgical oncology*, 11, p. 141.

Zhang, J. *et al*. (2003) 'Identification of the haematopoietic stem cell niche and control of the niche size', *Nature*, 425(6960), pp. 836–841.

Zhu, J. *et al*. (2018) 'HIF-1α promotes ZEB1 expression and EMT in a human bladder cancer lung metastasis animal model', *Oncology letters*, 15(3), pp. 3482–3489.

Zovein, A.C. *et al*. (2008) 'Fate tracing reveals the endothelial origin of hematopoietic stem cells', *Cell stem cell*, 3(6), pp. 625–636.